# Supporting Information

to

# Structural Principles to Steer the Selectivity of the Electrocatalytic Reduction of Aliphatic Ketones on Platinum

C. J. Bondue [a], F. Calle-Vallejo [b], M. C. Figueiredo [a], M. T. M. Koper [a,]

[a] Leiden Institute of Chemistry, Leiden University, P.O. Box 9502, 2300 RA Leiden, The Netherlands.

[b] Departament de Ciència de Materials i Química Fisica & Institut de Química Teòrica i Computacional (IQTCUB), Universitat de Barcelona, Martí i Franquès 1, 08028 Barcelona, Spain.

***Supplementary Note 1. Comparison Between CVs in Blank Electrolyte and in Acetone-Containing Electrolyte of Stepped Pt(111) Electrodes***

In Supplementary Figures 1 to 6 we compare CVs obtained at Pt(111), Pt(15,15,14), Pt(554), Pt(553), Pt(331) and Pt(110) in an electrolyte of 0.1 M $H_2SO_4$ (black curves) with those obtained at the same electrodes in an electrolyte of 0.1 M $H_2SO_4$ that contains 100 mM acetone (red curve).

The black CV in Supplementary Figure 1 has a large spike at 0.5 V in both the negative and positive going direction. This spike is associated with the rearrangement of the sulfate adlayer from a disordered structure (at potentials lower than that of the spike) to a $\left(\sqrt{3}\times\sqrt{7}\right)R19.1°$ superstructure (at potentials larger than the spike) at (111) terraces. Rather large (111) terraces are required to observe the sulfate spike, as evident from the black CV in Supplementary Figure 2. The introduction of (110) steps in the (15,15,14) surface limits the (111) terrace length to 30 atoms. This reduces the sharpness of the sulfate spike considerably. A similar effect is introduced by adsorbates: already a very small coverage with any adsorbate at Pt(111) suppresses the sulfate spike. The finding that the sulfate spike is still observable at both Pt(111) and Pt(15,15,14) electrodes despite the presence of 100 mM acetone (red curves in Supplementary Figures 1 and 2) is a strong indication that acetone does not adsorb on (111) terraces of platinum electrodes.

As we introduce (110) steps into the Pt(111) electrode a peak appears in the CV at 0.12 V (black curves in Supplementary Figure 2, 3, 4, 5, 6). This peak is associated with the adsorption (and desorption) of hydrogen at (110) step sites and grows accordingly as the step density increases. In the presence of acetone the peak due to hydrogen adsorption at Pt(110) step sites is suppressed in the negative going sweep (red curves in Supplementary Figures 2, 3, 4, 5 and 6). Hence, another

adsorbate (*i.e*. acetone) occupies the (110) steps. Only after reductive stripping of the adsorbed acetone at 0.05 V hydrogen can adsorb on the surface (indicated by the desorption of hydrogen at 0.12 V in the positive going sweep). Therefore, we conclude that the Pt(110) steps are the active sites of acetone reduction at Pt[(n-1)(111)x(110)] electrodes.

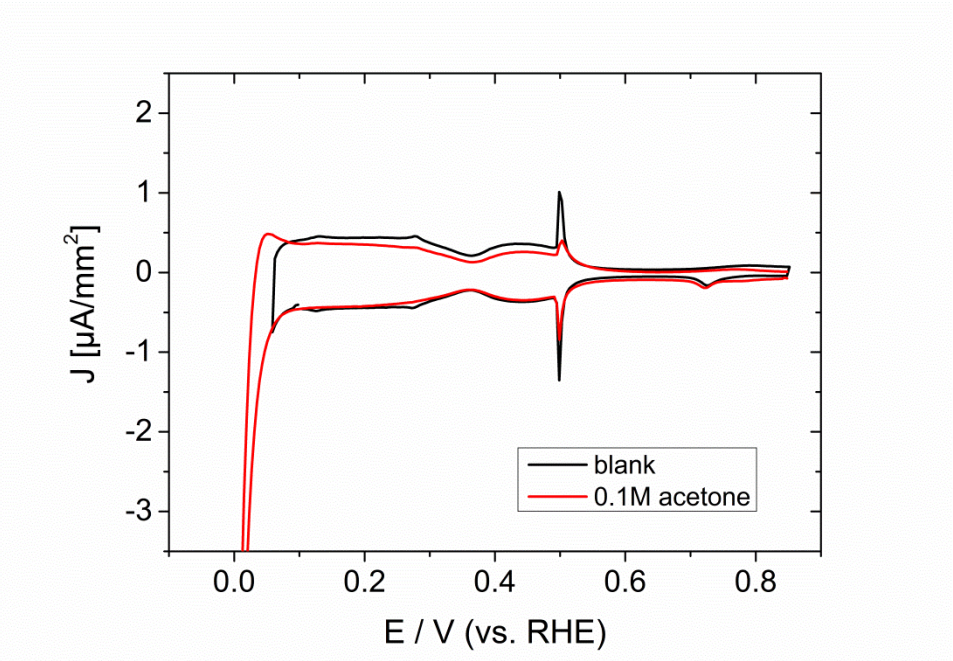


**Supplementary Figure 1. CV at Pt(111) in the presence of acetone.** Electrolyte: 0.1 M $H_2SO_4$ containing 0.1 M acetone. Sweep rate: 0.05 V/s.

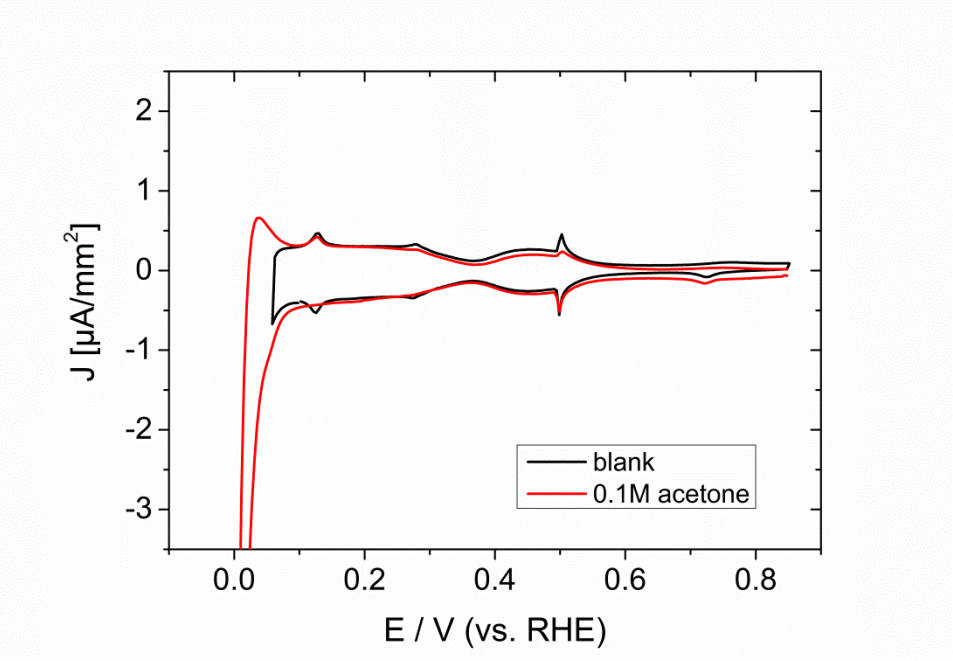


**Supplementary Figure 2. CV at Pt(15,15,14) in the presence of acetone.** Electrolyte: 0.1 M $H_2SO_4$ containing 0.1 M acetone. Sweep rate: 0.05 V/s.

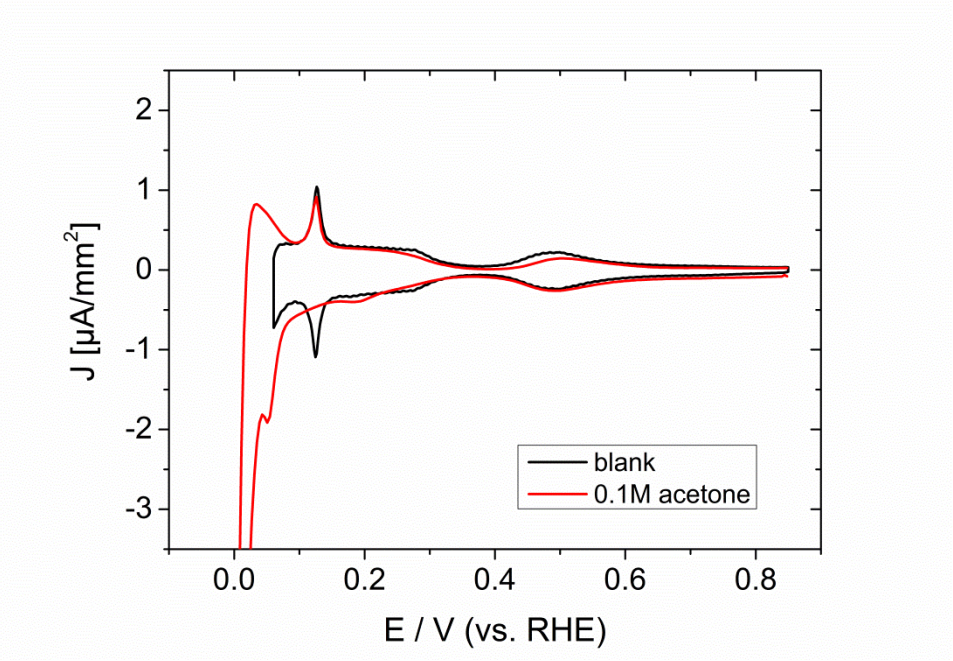


**Supplementary Figure 3. CV at Pt(554) in the presence of acetone.** Electrolyte: 0.1 M $H_2SO_4$ containing 0.1 M acetone. Sweep rate: 0.05 V/s.

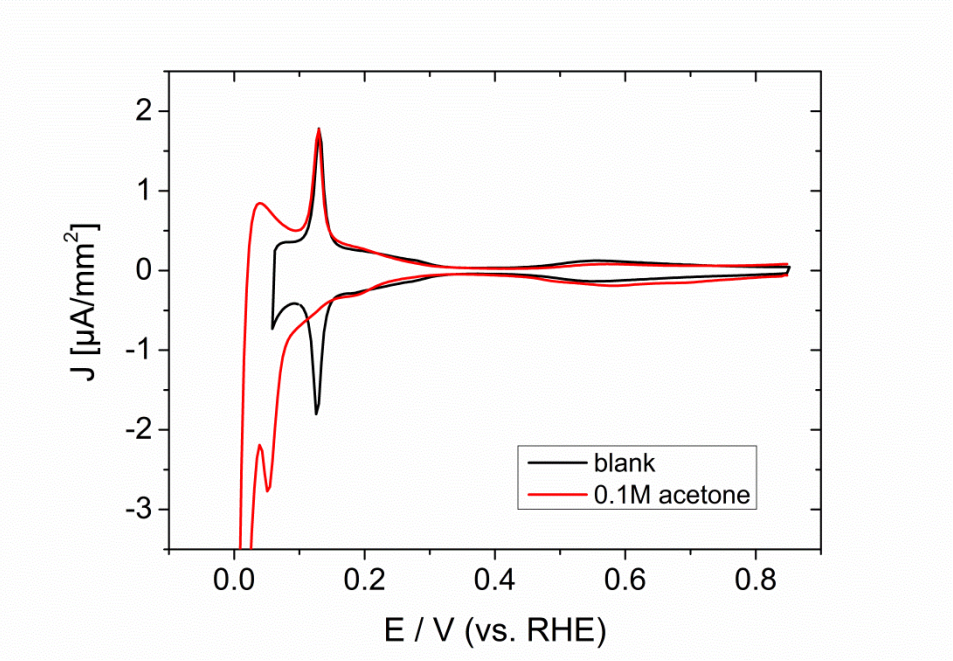


**Supplementary Figure 4. CV at Pt(553) in the presence of acetone.** Electrolyte: 0.1 M $H_2SO_4$ containing 0.1 M acetone. Sweep rate: 0.05 V/s.

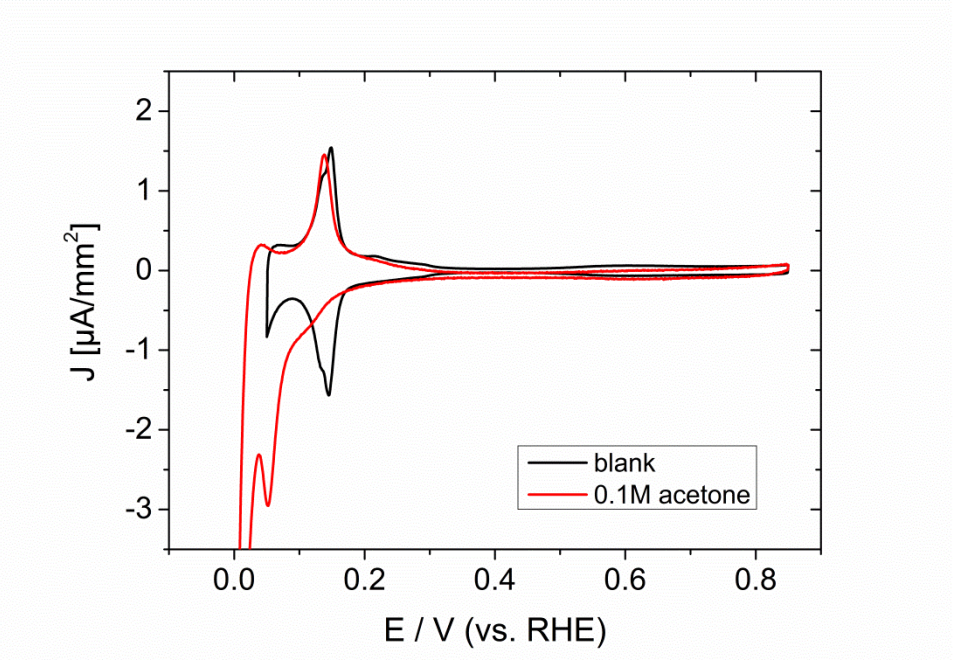


**Supplementary Figure 5. CV at Pt(331) in the presence of acetone.** Electrolyte: 0.1 M $H_2SO_4$ containing 0.1 M acetone. Sweep rate: 0.05 V/s.

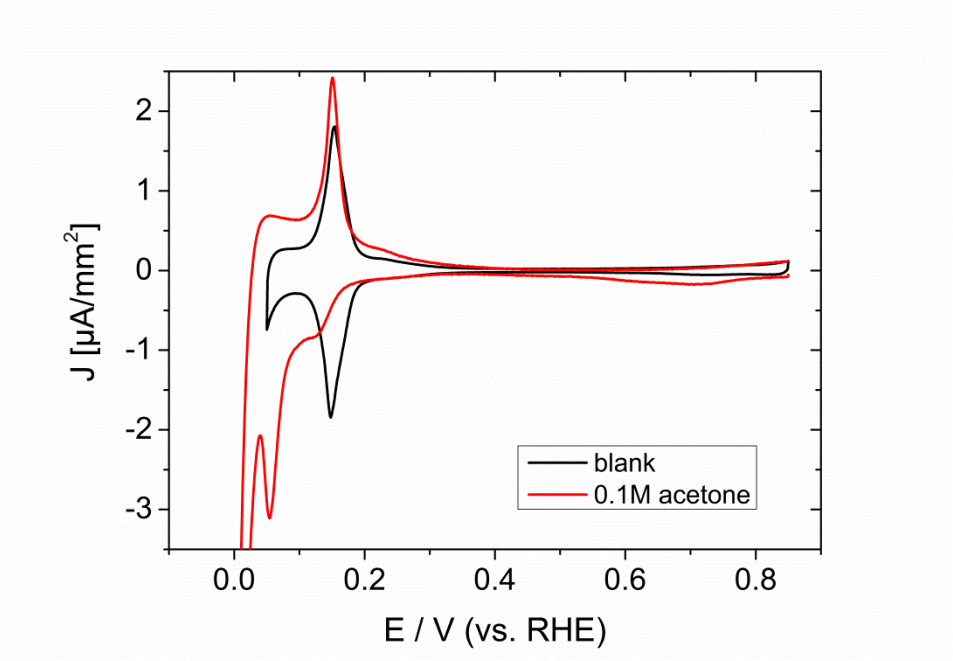


**Supplementary Figure 6. CV at Pt(110) in the presence of acetone.** Electrolyte: 0.1 M $H_2SO_4$ containing 0.1 M acetone. Sweep rate: 0.05 V/s.

***Supplementary Note 2. Proof for the Adsorption of Acetone at (110) Step Sites at Potentials Between 0.6 V and 0.4 V***

Supplementary Figure 7A shows the CV at Pt(553) in an electrolyte of 0.1 M $H_2SO_4$ containing $2 \times 10^{-4}$ M acetone. Prior to the first potential sweep, the electrode was kept at 0.15 V for 15 minutes. No potential stop was conducted prior to the second potential sweep. In the second potential sweep (red curve in Figure 3) a reversible peak at 0.12 V indicates the adsorption/desorption of hydrogen from the Pt(110) steps. The peak at 0.05 V, indicative for acetone reduction, is missing. In the first cycle, however, the peak due to hydrogen adsorption is suppressed, while acetone reduction proceeds at 0.05 V. The peak due to hydrogen desorption in the positive-going scan is not affected.

The results in Supplementary Figure 7A show that there is a competition between hydrogen and acetone adsorption. The fact that acetone reduction is observed in the first potential sweep

reveals that acetone accumulates on the platinum surface during the 15 minutes in which the potential is fixed at 0.15 V. The observation that adsorbed acetone suppresses hydrogen adsorption at 0.12 V shows that it adsorbs at (110) steps. Once all the acetone is removed from the electrode, hydrogen can adsorb at the electrode again.

The same observation as in Supplementary Figure 7A can be made in Supplementary Figure 8B where the potential was held at 0.2 V. However, barely any acetone reduction is observed in Supplementary Figure 7C where the potential was held at 0.4 V prior to the experiment. This indicates that hardly any acetone accumulates at the surface at 0.4 V. During the potential stop at 0.6 V no acetone adsorbs at the surface, since no reduction is observed. Hence, acetone adsorption starts to take place in the potential region between 0.4 V and 0.6 V.

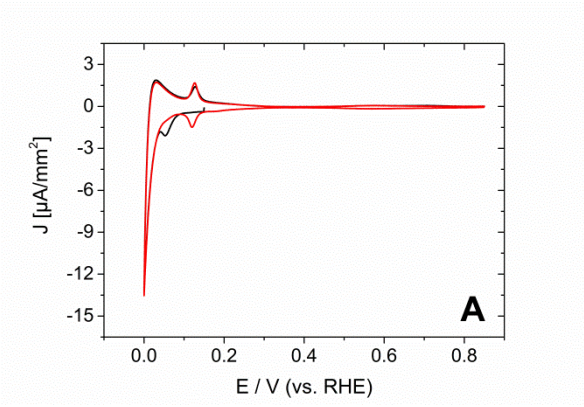


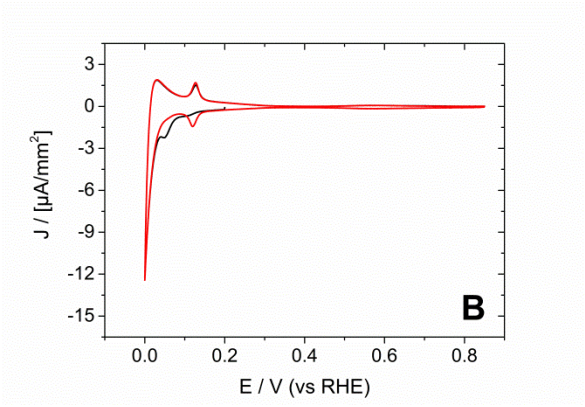

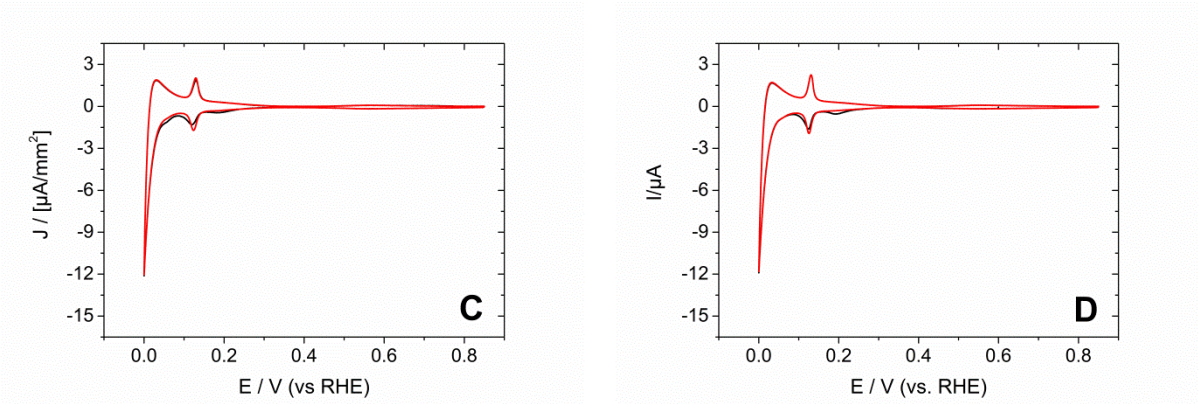


**Supplementary Figure S7. Potential dependent adsorption of acetone.** CV at Pt(553) in 0.1 M $H_2SO_4$ containing 200µM acetone. Black: first potential sweep, red: second potential sweep. Prior to the first sweep the potential was held at the start potential for 15 minutes. Sweep rate: 0.05 V/s; A: $E_{start}$ = 0.15 V; B: $E_{start}$ = 0.2 V; C: $E_{start}$ = 0.4 V; D: $E_{start}$ = 0.6 V.

***Supplementary Note. 3 Activity of Stepped Pt(111) Electrodes: the Effect of Real Step Density***

In Figure 1B we have plotted the current density at 50 mV in an acetone containing electrolyte as the function of nominal (110) step density. However, the nominal step density can deviate from the real step density. This is particularly true for Pt(110) where the (2x1) reconstruction reduces the real step density with respect to the nominal value. Therefore, we have plotted the current density obtained at 50 mV in the presence of 100 mM of acetone versus the surface concentration of step atoms ($\Gamma_{AtepAatom}$). That has been calculate from Supplementary Equation 1 from the charge due to hydrogen desorption $Q_{H-UPDatA(110)}$. The latter was determined from the respective CVs in Supplementary Figures 1 to 6. F in Equation one is Faradays constant and A is the surface area of the electrode.

$$\Gamma_{step\ atom} = \frac{Q_{H-UPD\ at\ (110)}}{\cdot F} \qquad \text{Eq. 1}$$

Qualitatively Supplementary Figure 8 and Figure 1 yield the same results: Whether plotted versus the theoretical step density or versus $\Gamma_{step\ atom}$ the current density due to acetone reduction

only increases linearly until a limiting value is achieve. The effect of the step density or of $\Gamma_{step\ atom}$ levels of, however, as the value determined for Pt(553) is exceeded. Pt(331) and Pt(110) have essentially the same activity, which is barely larger than that of Pt(553).

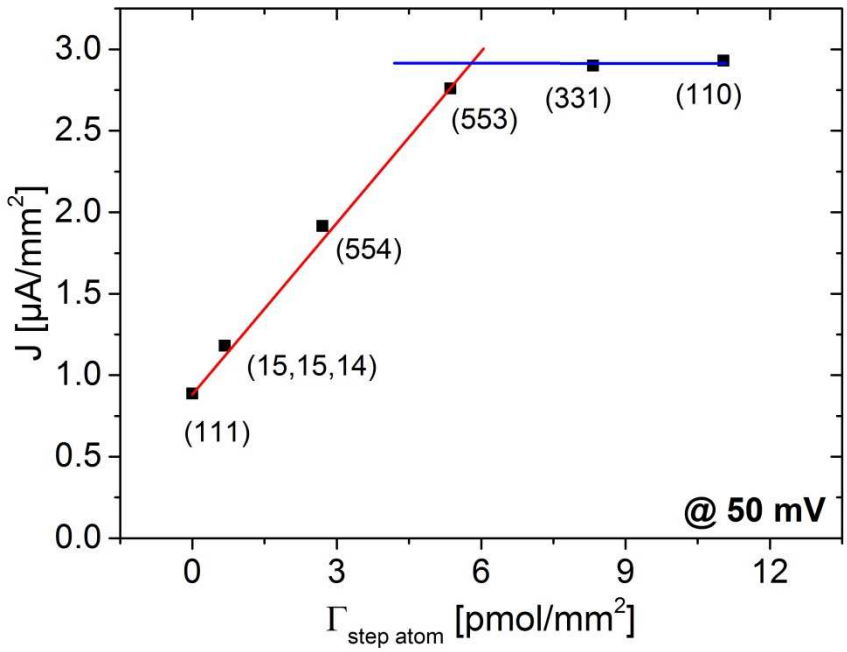


**Supplementary Figure S8**. **Influence of the true step density of Pt[(n-1)(111)x(110)] electrodes on acetone reduction:** Current density (values as in Figure 1B) at 50 mV plotted as a function of the surface concentration of step atoms of the respective electrodes. The surface concentration of step atoms was determined from the charge due to hydrogen desorption form step sites in the CVs of Figures S1 to S6 (black curves).

***Supplementary Note 4. Stability Upon Cycling of Pt(553) and Pt(510)***

Supplementary Figure 9 shows the CVs obtained at Pt(553) and Pt(510) electrodes in an electrolyte of 0.1 M $H_2SO_4$ that contains 100 mM of acetone. The 19$^{th}$ cycle at the Pt(553) electrode does not differ significantly from the first 3 cycles. In particular, the peak at 0.05 V in the negative going sweep, which has been associated with acetone reduction, is still present. The situation is different for the Pt(510) electrode: the shoulder prior to hydrogen evolution due to acetone reduction declines from cycle to cycle. Already in the 3$^{rd}$ cycle barely any activity for acetone reduction is left. Different from the Pt(553) electrode, catalyst poisons form and accumulate at the Pt(510) electrode in the presence of acetone. In general Pt[(n-1)(111)x(110)]-type electrodes do not undergo poisoning while Pt[(n+1)(100)x(110)]-type electrodes do.

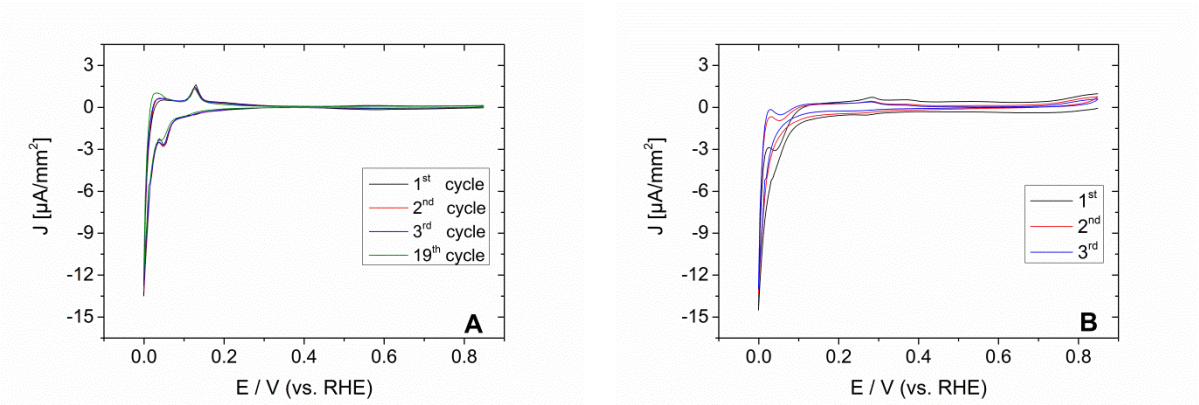


**Supplementary Figure 9. Evolution of the CVs with cycle number.** CV at Pt(553) (A) and Pt(510) (B) in 0.1 M $H_2SO_4$ containing 0.1 M acetone. Sweep rate: 0.05 V/s

***Supplementary Note 5. Comparison Between CVs in Blank Electrolyte and in Acetone-Containing Electrolyte of Stepped Pt(100) Electrodes***

In Supplementary Figures 10 to 12 we compare CVs obtained at Pt(100), Pt(10,1,0) and Pt(510) in an electrolyte of 0.1 M $H_2SO_4$ (black curves) with those obtained at the same electrodes in an electrolyte of 0.1 M $H_2SO_4$ that contains 100 mM acetone (red curve).

The reversible peak in the black curves of Supplementary Figures 10, 11 and 12 at 0.4 V is due to the adsorption (negative going sweep) and desorption (positive going sweep) of hydrogen at (100) terraces. At the stepped platinum electrodes (i.e. Pt(10,1,0) and Pt(510)) a second reversible peak appears at 0.28 V. This peak is due to the adsorption and desorption of hydrogen at the step edges. In the red curve of Supplementary Figure 10, corresponding to Pt(100), hydrogen adsorption is suppressed in the presence of 100 mM acetone. This is due to the fact that the sites for hydrogen adsorption are already occupied by an adsorbate. As the potential is decreased into the potential region of hydrogen evolution no additional reduction process is visible despite the presence of an adsorbate at Pt(100). In the positive going sweep barely any desorption of hydrogen from the (100) terraces is observed. Hence, the adsorbate was not stripped reductively during the sweep into the hydrogen evolution region, which would have allowed the adsorption of hydrogen. Therefore, it can be concluded that the adsorbate is still present at the surface. Hence, no or barely any reduction process occurs at pristine Pt(100) electrodes, suggesting that Pt(100) terraces are inactive for the acetone reduction. The adsorbate formed (100)-terraces is only removed oxidative in a broad peak between 0.7 V and 0.85 V in the positive going sweep. As pointed out in the main article the adsorbate formed at the pristine (100)-electrode is not identical with acetone. Indeed, computational

modelling shows that it is thermodynamically unfavorable for acetone to adsorb at Pt(100) electrodes (c.f. Inset of Figure 6A and related discussion). The adsorbat is rather the result of incomplete acetone oxidation occurring at potential smaller 0.7 V at Pt(100) terraces (c.f. Figure 2B and related discussion).

The situation is somewhat different in the red curves of Supplementary Figures 11 and 12, corresponding to the stepped electrodes. There, hydrogen adsorption is also suppressed in the negative going sweep at both terrace sites and step sites. As the potential is reduced into the region of hydrogen evolution a shoulder at 0.05 V indicates a reduction process at the stepped platinum surfaces. In the subsequent positive going sweep still no hydrogen desorption is observed at the (100) terraces. Hence, also at the stepped surfaces the adsorbate is not stripped from the (100) terraces. However, a peak at 0.28 V due to hydrogen desorption at the step sites is observed in the positive going sweep of the red curves in Supplementary Figures 11 and 12. This indicates that the adsorbate at the step sites is reductively stripped during the sweep into the potential region of hydrogen evolution and hydrogen was allowed to adsorb at the steps. This corroborates the finding of DFT calculations that the reduction of acetone takes place at the step sites of Pt[(n+1)(100)x(110)]-type electrodes.

Also in the CV at Pt(10,1,0) and Pt(510) an oxidation current is observed in the positive going sweep between 0.7 V and 0.85 V. The current density due to this oxidation process decreases as the (100) terrace size decreases. DFT calculations show that acetone does not molecularly adsorb on the (100) terraces of platinum. However, we have shown in Figure 2B that acetone is oxidized at the (100) terraces and that fragments of acetone oxidation remain adsorbed on the surface, and they can only be stripped off in the potential region between 0.7 V and 0.85 V.

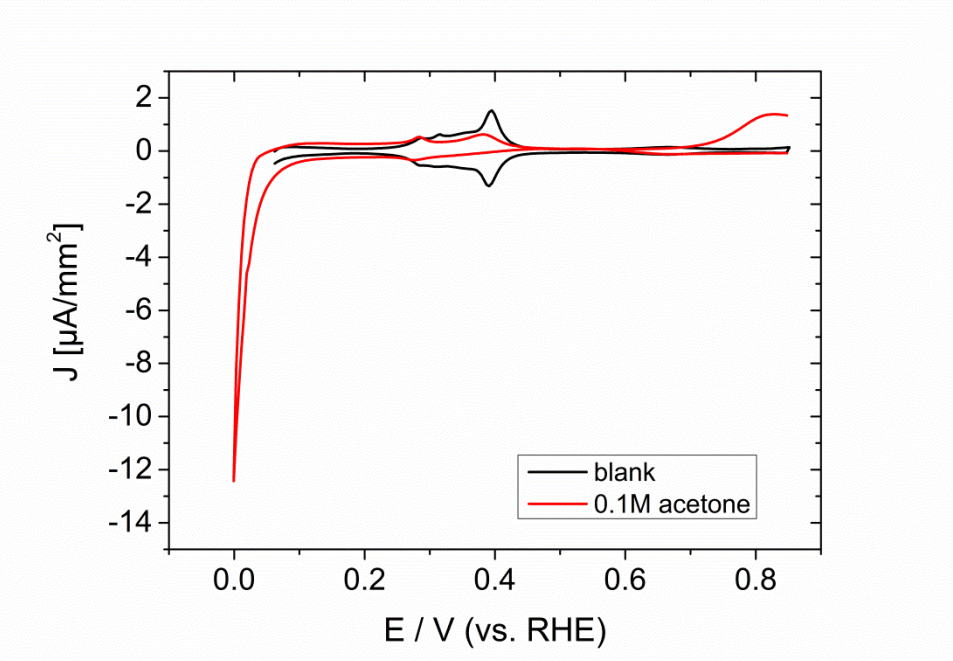


**Supplementary Figure 10. CV at Pt(100) in the presence of acetone.** Electrolyte: 0.1 M $H_2SO_4$ containing 0.1 M acetone. Sweep rate: 0.05 V/s.

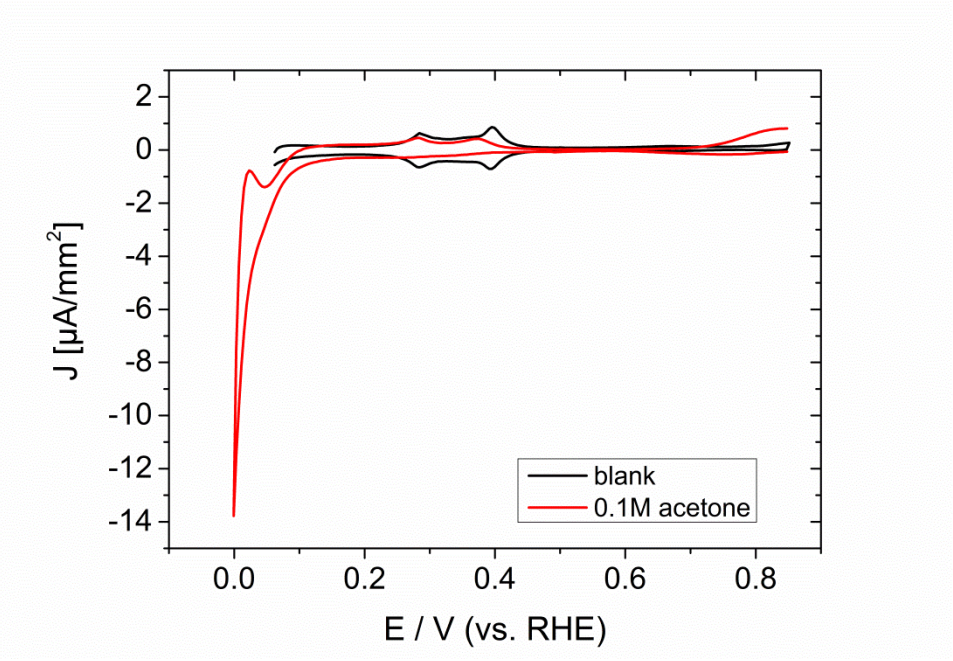


**Supplementary Figure 11. CV at Pt(10,1,0) in the presence of acetone.** Electrolyte: 0.1 M $H_2SO_4$ containing 0.1 M acetone. Sweep rate: 0.05 V/s.

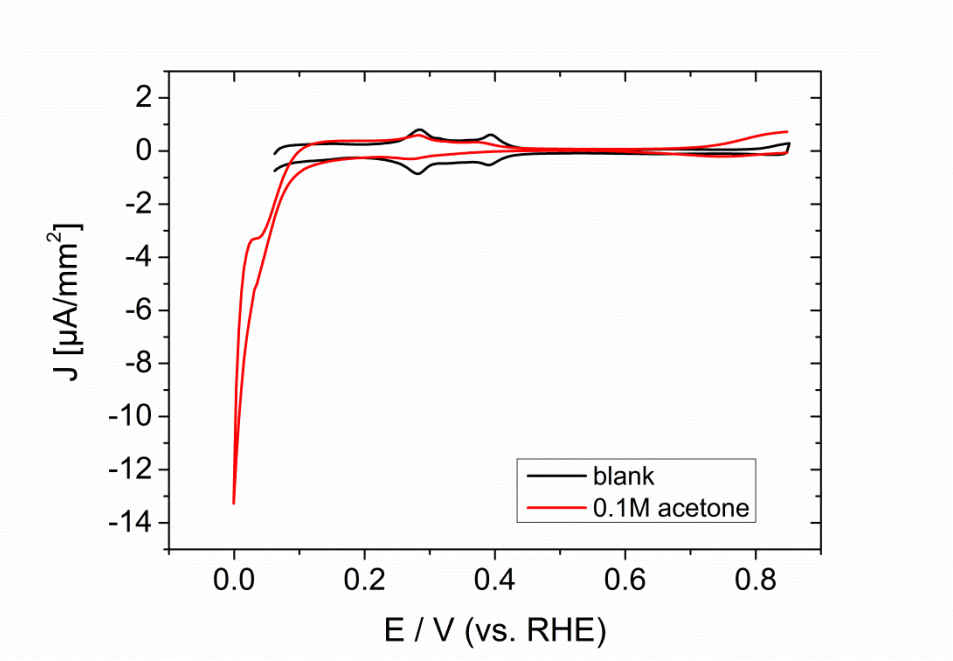


**Supplementary Figure 12. CV at Pt(510) in the presence of acetone.** Electrolyte: 0.1 M $H_2SO_4$ containing 0.1 M acetone. Sweep rate: 0.05 V/s.

***Supplementary Note 6. Effect of Accumulated Acetone Fragments on Acetone Reduction at Pt(510)***

It is shown in Figure 2B that acetone is oxidized at (100) terraces at potentials more negative than 0.7 V. Fragments of incomplete acetone reduction remain bound to the surface and are stripped off only at potentials more positive than 0.7 V. In Supplementary Figure 13 we show the effect of adsorbed acetone fragments on acetone reduction at Pt(510). In the black curve, we kept the potential for 2 minutes at 0.85 V where no acetone oxidation takes place. After that we conduct a linear swept with a sweep rate of 0.05 V/s into the potential region to 0 V. A large negative current at 0 V in the negative going sweep indicates hydrogen evolution. Prior to hydrogen evolution at 0.05 V a shoulder appears, which can only be observed in the presence of acetone and which, therefore, indicates acetone reduction (black curve).

Prior to the recording of the red curve in Supplementary Figure 13 we kept the Pt(510) electrode for 2 minutes at 0.45 V. At 0.45 V the electrode accumulates fragments of incomplete acetone oxidation. After the potential stop a linear sweep to 0 V is performed. At roughly 0.1 V in the negative going sweep the current begins to decrease monotonously, as expected for hydrogen evolution. The shoulder at 0.05 V observed in the black curve of Supplementary Figure 13 is missing indicating that acetone reduction is suppressed. Based on that it can be concluded that accumulation of fragments of incomplete acetone oxidation results in the deactivation of the electrode.

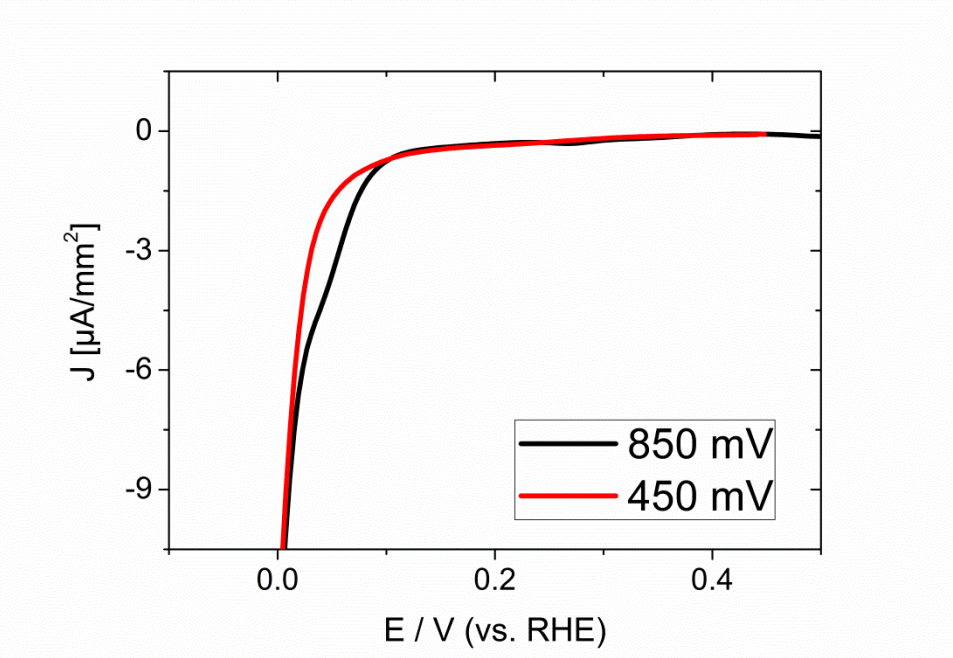


**Supplementary Figure 13. Potential dependence of electrode poisoning.** CV at Pt(510) in an electrolyte of 0.1 M $H_2SO_4$ containing 0.1 M acetone after holding the potential for 2 minutes at the indicated value. For clarity, only the negative-going sweep is shown. Sweep rate: 0.05 V/sec.

***Supplementary Note 7. SERS-Spectra of adsorbed Acetone***

Supplementary Figure 14 shows Surface Enhance Raman Spectra (SERS) obtained at polycrystalline platinum in an electrolyte of 0.1 M $H_2SO_4$ containing 10 mM of acetone. The absence at 800 mV of bands indicates that no adsorbate is present. However, as soon as the potential is stepped to 400 mV three bands of moderate intensity appear at 1538 $cm^{-1}$, 1592 $cm^{-1}$ and 2920 $cm^{-1}$ indicating that acetone adsorption takes place at this potential. This is in good agreement with the results obtained from the CV-data in Supplementary Figure 7 showing that acetone adsorption takes place in the potential range between 0.6 V and 0.4 V.

The band at 2920 $cm^{-1}$ can be assigned to the symmetric stretching vibration of the methyl group and is barely shifted with respect to the vibration mode of free acetone[1]. Since adsorption has barely any influence on the C,H-binding strength of the methyl groups, adsorption is unlikely to proceed through the methyl groups.

The other two bands are more difficult to assign: free acetone features no bands in the frequency region between 1600 $cm^{-1}$ and 1500 $cm^{-1}$ [1]. The bands of free acetone nearest to this frequency region are the C,O-stretch vibration located at 1710 $cm^{-1}$ [1] and the asymmetric scissoring vibration of the methyl groups located at 1435 $cm^{-1}$ [1]. There is no obvious reason why adsorption of acetone should render the asymmetric scissoring vibration more difficult and shift it, therefore, by 100 $cm^{-1}$ to higher energies.

As adsorption does not proceed through the methyl groups acetone has to adsorb either via the carbonyl carbon or the carbonyl oxygen. It is, therefore, plausible that acetone adsorption weakens the C,O-bond and shifts the C,O-stretch vibration to lower wave numbers. Hence, it is not unexpected that we find a band due to the C,O-stretch vibration in the frequency range between 1500 $cm^{-1}$ and 1600 $cm^{-1}$. In addition computational modeling shows that acetone adsorption strength depends significantly on the normalized coordination number of the surface site (inset Figure 6). We assign the two bands a 1538 $cm^{-1}$ and 1592 $cm^{-1}$ in the SERS spectra to the C,O-stretch

vibration of acetone adsorbed at two different crystallographic sites of the polycrystalline platinum electrode, where the C,O-binding strength is weakened to different degrees.

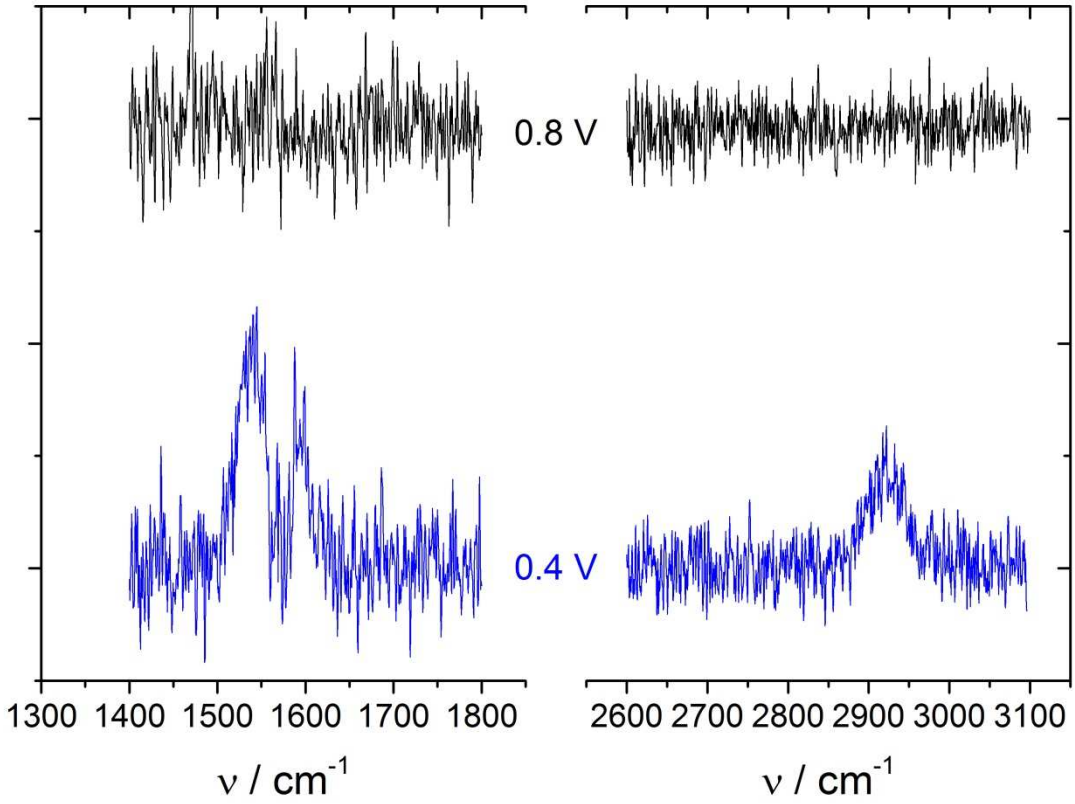


**Supplementary Figure 14. SERS-spectra obtained at polycrystalline platinum in an electrolyte of 0.1 M $H_2SO_4$ that contained 10 mM acetone.**

Experimental: Platinum was deposited galvanostatically with a current density of 400 µA for 20 seconds from an electrolyte of 0.35 M $H_3PO_4$ containing 100 µM $H_2PtCl_6$. Prior to this procedure the gold electrode was roughened in an electrolyte of 0.5 M KCl by repeated cycling between -0.4 V and 1.2 V (versus Ag/AgCl) until a roughness factor of approximately 3 was achieved. The electrode prepared in such a way was transferred to the RAMAN cell that is described elsewhere [2]. The Raman spectra were collected with a LabRam HR800 (Horiba Jobin Yvon) confocal microscope that was equipped with an HeNe-Laser (632.81 nm).

**Supplementary Note 8. Additional Computational Modelling**

PBE has proven reliable to model reactions within the carbon cycle. In particular, we highlight the good agreement obtained in our previous studies between theory and experiments for dimethyl ether oxidation to $CO_2$ [3] acetaldehyde reduction to ethanol [4], and CO reduction to ethylene [5]. Following the work of Peterson et al [6] and our own work [7], to guarantee that the predicted and experimental standard equilibrium potentials be (nearly) identical we make corrections to gas-phase substances via error analysis of thermochemical data. In this case, the total energy of acetone is corrected by 0.08 eV and those of 2-propanol and propane by -0.05 eV.

Supplementary Table 1 contains the solvation corrections used for the adsorbates in this study. For *OH we took the value reported in ref.[7] on pure Pt, whereas for adsorbed acetone and *R-OH we took the value reported in ref.[8] of -0.38 eV calculated for *COH and modified it based on steric hindrance by multiplying by 1/3 or 2/3.

**Supplementary Table 1.** Solvation corrections for various adsorbates in Supplementary Figure 15. Those which do not appear in the table are not considered to be stabilized by solvation.

| species | adsorbate ID | $E_{solvation}$ | Ref |
|---|---|---|---|
| *OH | G | -0.58 | 1 |
| *$CH_3$-CO-$CH_3$ | B | -0.13 | 2 |
| *$CH_3$-C(OH)-$CH_3$ | C | -0.13 | 2 |
| *O-CH-$CH_3$-$CH_3$ | E | -0.25 | 2 |
| *$CH_2$-C(OH)-$CH_3$ | B | -0.13 | 2 |
| *$CH_2$-CH(OH)-$CH_3$ | F | -0.25 | 2 |

In Supplementary Table 2 we provide the adsorption energies ($\Delta G$) of all adsorbates in Supplementary Figure 15A on all sites under study (see Supplementary Figure 16), which were used to build the coordination-activity plots shown in Figures 6 and 7 in the main paper. Likewise, Supplementary Table 3 contains the energies required to evaluate the reaction network in Supplementary Figure 15B. The references for the adsorption energies are acetone and propenol, respectively.

**Supplementary Table 2.** Adsorption energies (in eV) for the adsorbates in Supplementary Figure 16A on the sites shown in Supplementary Figure 17.

| adsorbate / site | $510E_1$ | 553E | 110E | $510E_2$ | 100T | 111T |
|---|---|---|---|---|---|---|
| $cn$ | 6 | 7 | 7 | 8 | 8 | 9 |
| $\overline{CN}$ | 4.92 | 5.50 | 5.83 | 6.25 | 6.67 | 7.50 |
| $*CH_3COCH_3$ | -0.45 | -0.29 | -0.10 | 0.11 | 0.44 | 0.68 |
| $*CH_3COHCH_3$ | -0.36 | -0.29 | -0.19 | -0.05 | 0.03 | 0.35 |
| $*CH_3CCH_3$ | -0.77 | -0.72 | -0.75 | -0.65 | -0.36 | -0.08 |
| $*CH_3CHCH_3$ | -0.88 | -0.67 | -0.67 | -0.58 | -0.54 | -0.26 |
| $*OCHCH_3CH_3$ | -0.03 | 0.17 | 0.28 | 0.54 | 0.28 | 0.86 |
| *O | -0.07 | 0.13 | 0.19 | 0.09 | 0.22 | 0.23 |
| *OH | -1.13 | -1.01 | -0.93 | -0.98 | -1.08 | -0.48 |
| $*OH + *CH_3\text{-}C\text{-}CH_3$ | -0.65 | -0.43 | -0.42 | - | 0.04 | 0.86 |
| $*OH + *CH_3\text{-}CH\text{-}CH_3$ | -0.84 | -0.34 | -0.25 | - | -0.22 | 0.84 |

**Supplementary Table 3.** Adsorption energies (in eV) for the adsorbates in S. Figure 16B on the sites shown in S. Figure 17.

| Adsorbate | 553E | $510E_1$ |
|---|---|---|
| $*CH_2\text{-}C(OH)\text{-}CH_3$ | -0.66 | -0.60 |
| $*CH_2\text{-}CH\text{-}CH_3$ | -1.25 | -1.25 |
| $*CH_2\text{-}CH_2\text{-}CH_3$ | -1.01 | -1.22 |
| $*CH_2\text{-}C\text{-}CH_3$ | -1.07 | -1.41 |
| $*CH_2\text{-}CH(OH)\text{-}CH_3$ | -0.38 | -0.46 |
| $*CH_3\text{-}C(OH)\text{-}CH_3$ | -0.70 | -0.75 |
| $*CH_3\text{-}C\text{-}CH_3$ | -1.13 | -1.18 |
| $*CH_3\text{-}CH\text{-}CH_3$ | -1.08 | -1.29 |

Supplementary Figures 15A and 15B contain the reaction networks considered for 2-propanol and propane production from acetone and propenol (the enol tautomer of acetone), respectively. The lowest-energy pathways from all those in Supplementary Figure 15 are shown in Figure 5 in the main paper and were used to build the coordination-activity plots in Figures 6 and 7 in the main paper. Note that the pathways in Supplementary Figure 15B were only evaluated for Pt(553) and Pt(510).

**A)**

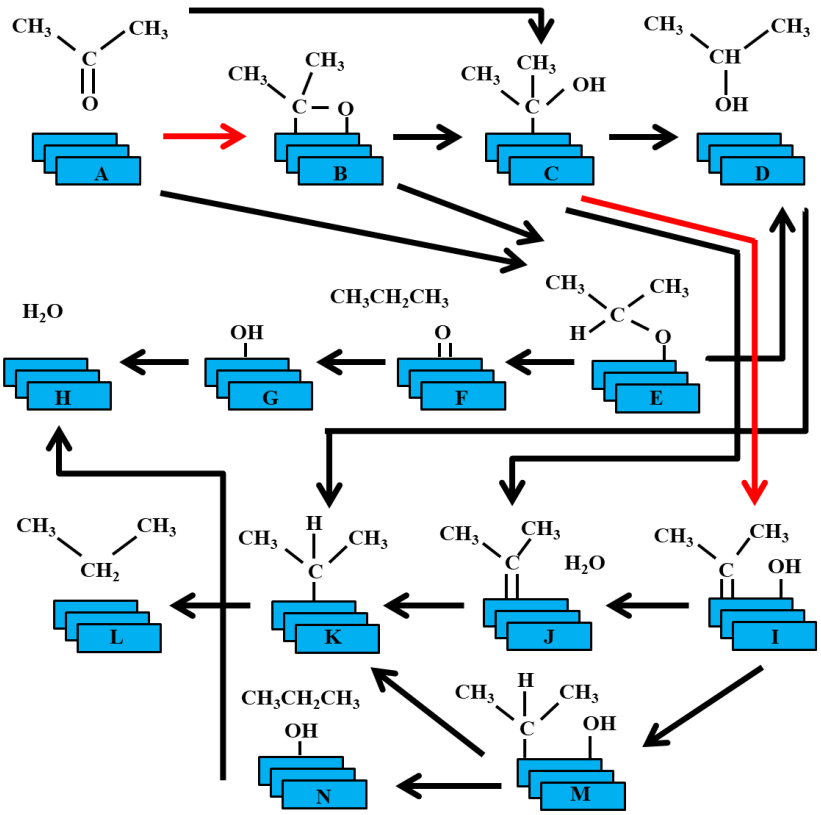


**B)**

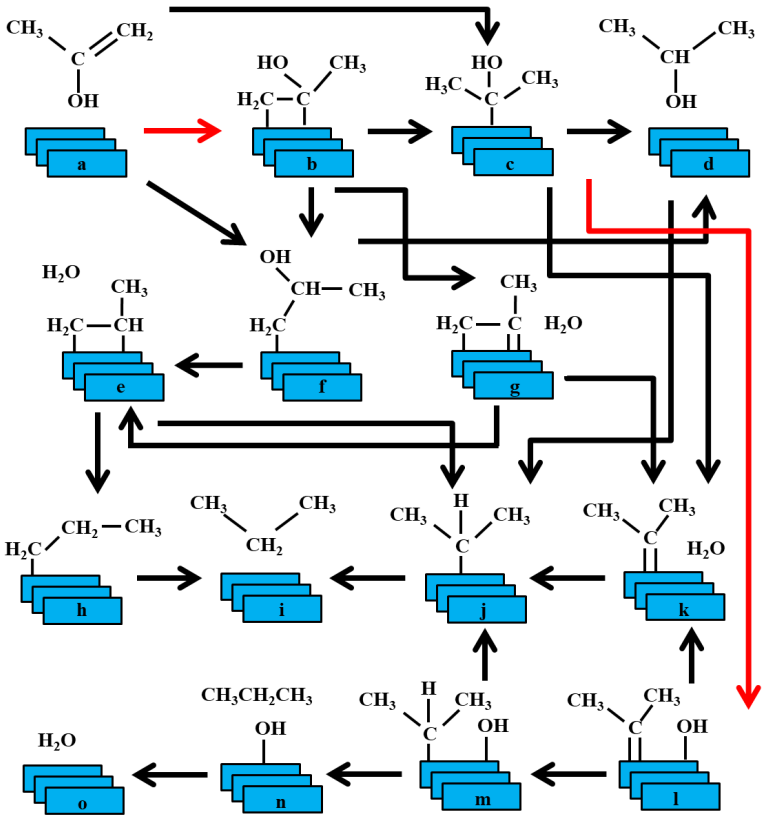

**Supplementary Figure 15. Reaction networks considered for the formation of 2-propanol and propane**. (A) formation from acetone and (B) formation from propenol, its enol tautomer. Black lines indicate electrochemical steps, whereas red lines indicate chemical steps.

Supplementary Figure 16 shows top views of the five surfaces simulated in this study, highlighting in yellow the active sites considered. The corresponding generalized coordination numbers are also provided.

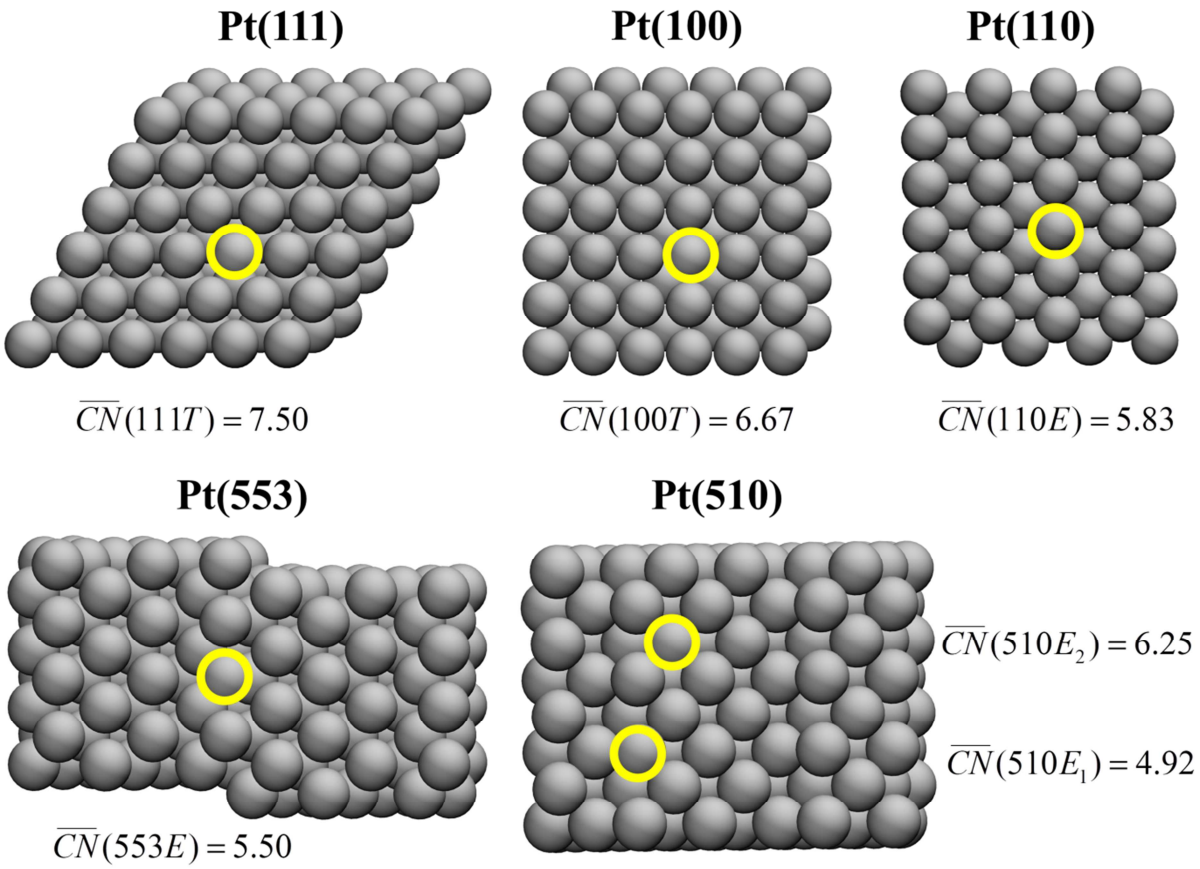


**Supplementary Figure 16. Surfaces and active sites under study.** 111T: (111) terrace site. 100T: (100) terrace site. 110E: step-edge site on Pt(110). 553E: step-edge site on Pt(553). 510E: step-edge site on Pt(510).

In Supplementary Figure 17 we show the free energy diagrams for Pt(553) and Pt(510) for the most favorable pathways when the reactant is not acetone but propenol (see Supplementary Figure 15B), its enol tautomer. The diagrams are made at the onset potentials for the preferred products, which are -0.02 V for 2-propanol on Pt(553) and 0.11 V for propane on Pt(510). Note that

the onset potentials are nearly the same when acetone is the reactant: -0.03 V for 2-propanol on Pt(553)and 0.11 V for propane production on Pt(510). It is also worth noting that the adsorbed reaction intermediates are identical to those in Figure 5 in the main paper.

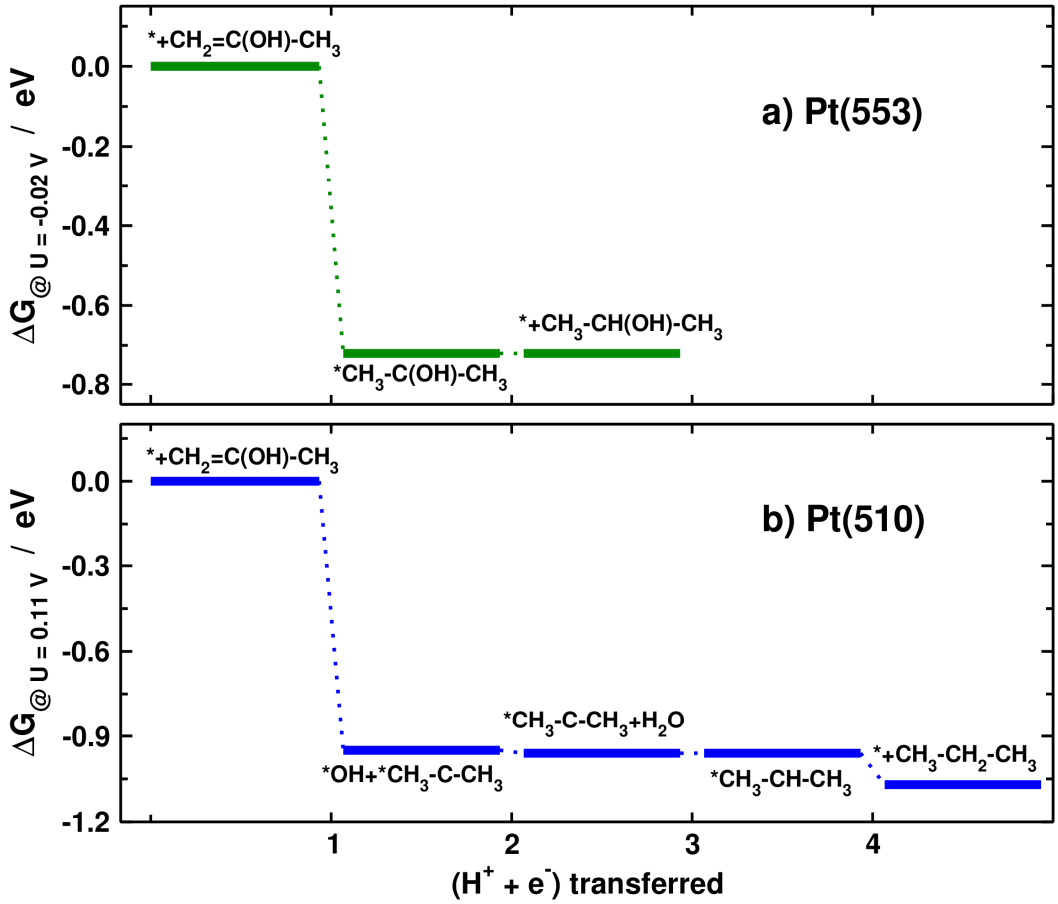


**Supplementary Figure S17. Free energy diagrams**. Diagrams for a) 2-propanol on Pt(553) and b) propane on Pt(510) when the reactant is propenol ($CH_2$=CH(OH)$CH_3$). The diagrams are provided at the onset potentials for the preferred products: -0.02 V for 2-propanol on Pt(553) and 0.11 V for propane on Pt(510).

In Supplementary Figure 18A we provide the linear relationships upon which the coordination-activity plots in Figure 6 in the main paper are based. In each case we provide the equation of the linear fit together with the mean absolute error (MAE) between the calculated data points and the fit. Supplementary Figure 18B collects some hydrogen adsorption data from this and previous work [9]. The figure shows an approximately linear relationship between the adsorption energies of hydrogen and $\overline{CN}$. Such behavior is in line with that of acetone adsorption (Figure 6A,

inset) and those of the reaction intermediates of acetone reduction (Supplementary Figure 18A). The inset of Supplementary Figure 18B shows that the lines for *H and *$CH_3COCH_3$ intersect at $\overline{CN} \approx 5.8$, which usually corresponds to undercoordinated defect sites. For sites with $\overline{CN} \leq 5.8$ acetone adsorption is stronger than *H.

**A)**

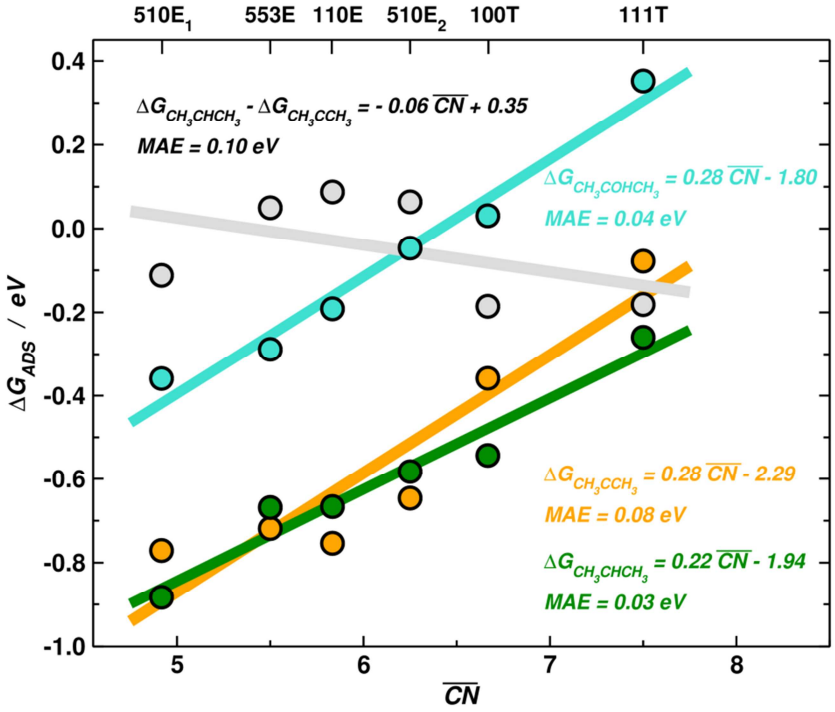


**B)**

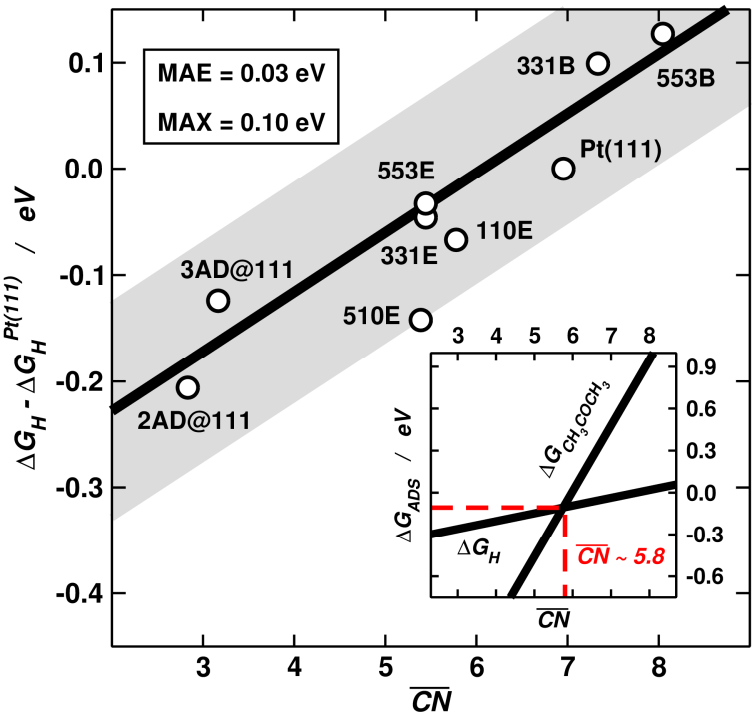


**Supplementary Figure 18. Relationship between generalized coordination number and adsorption energies.** Linear relationships between $\overline{CN}$ and A) the adsorption energies of selected intermediates of acetone reduction on Pt, and B) *H with respect to Pt(111). The data in (B) are taken from this study and a previous work [9] Inset: The linear fits for hydrogen and acetone adsorption are used to determine that $*CH_3COCH_3$ is more stable than *H for sites with $\overline{CN} \leq 5.8$. MAE, MAX: Mean/ maximum absolute errors between the linear fits and the data points. E: step edges, B: step bottoms.

### *Supplementary Note 9. Role of Alcohols During Ketone Reduction*

Supplementary Figure 19 compares the CVs at Pt(510) obtained in the blank electrolyte of 0.1 M $H_2SO_4$ (black curve), with the CVs obtained in the presence of 0.2 M 2-propanol (red curve) and in the presence of both 0.2 M 2-propanol and 0.1 M acetone (blue curve). As 2-propanol is added to the blank electrolyte no additional current is observed. Hence, Pt(510) is not capable of reducing 2-propanol to the hydrocarbon. In order to show the presence of 2-propanol does not simply result in the poisoning of the electrode we also collected the blue curve in Supplementary Figure 19: it shows that the reduction of acetone at Pt(510) is not impaired by the presence of 0.2 M 2-propanol. Hence, the lack of activity for 2-propanol reduction is due to an inherent inability of the electrodes to reduce the alcohol to the corresponding hydrocarbon under these conditions. This finding is interesting as it

shows that alcohols are not intermediates in the reduction of aliphatic ketones to hydrocarbons, in line with the pathways in Figure 5, at least not on single crystals under the employed conditions.

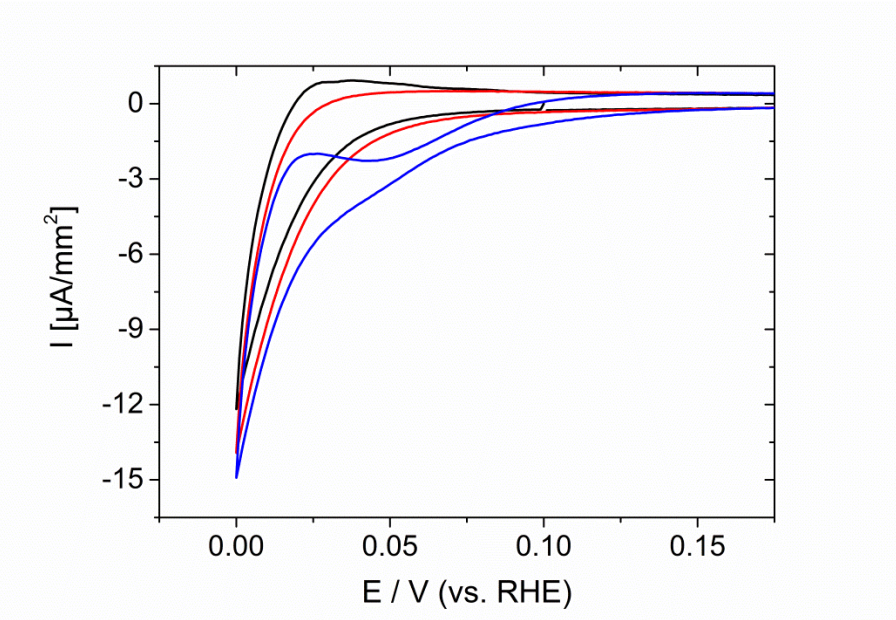


**Supplementary Figure 19. Role of Propanol in the course of acetone reduction.** CV at Pt(510) in an electrolyte of 0.1 M $H_2SO_4$ (black), 0.1 M $H_2SO_4$ containing 0.2 M 2-propanol (red), and 0.1 M $H_2SO_4$ containing 0.2 M 2-propanol and 0.1 M acetone. Sweep rate: 0.05 V/s. Potential limits: 0 V to 0.85 V.

### *Supplementary Note 10. Comparison Between Acetone, Butanone and 3-Pentanone*

Supplementary Figures 20 – 28 show the CVs at Pt(111), Pt(15,15,14), Pt(554), Pt(553), Pt(331), Pt(110), Pt(100), Pt(10,1,0) and Pt(510) in the blank electrolyte (black curve) and in an electrolyte that contains 40 mM of acetone (part A in each figure), butanone (part B) and 3-pentanone (part C). The findings for butanone and 3-pentanone is essentially the same as those discussed for acetone in Sections I and IV of this Supporting Information. All ketones adsorb at the step sites of both Pt[(n-1)(111)x(110)]-type and Pt[(n+1)(100)x(110)]-type electrodes. This is clear from the suppression of hydrogen adsorption at step sites in the negative going sweep. The ketones are stripped reductively at approximately 0.05 V in a shoulder or a peak. This can be inferred from

the hydrogen desorption, that is largely unaffected by the presence of the ketone. In other words, in order to desorb hydrogen it has to adsorb at some point, but this is only possible once the ketones that blocked the step sites for hydrogen adsorption are stripped reductively.

All ketones form also an adsorbate at (100) terraces. This adsorbate is not stripped off in the potential range of hydrogen evolution and is still present in the positive going sweep. As in the case of acetone, the adsorbate formed at the (100) terrace is oxidized in the potential range between 0.7 V and 0.85 V.

The CVs obtained in butanone and 3-pentanone containing electrolyte are somewhat different from those obtained in acetone containing electrolyte: It was discussed above that the presence of the sulfate spike in acetone containing electrolyte indicates the absence of acetone adsorption. Butanone and 3-pentanone, however, suppress the sulfate peak in the positive going sweep. This indicates that butanone and 3-pentanone interact to some degree with the (111) terraces of platinum electrodes. However, since hydrogen adsorption is not or barely affected, the interaction is weak compared to the interaction with the step sites.

Supplementary Figure 29 combines all CVs obtained at Pt[(n-1)(111)x(110)]-type electrodes in ketone containing electrolyte. Supplementary Figure 30 does the same for Pt[(n+1)(100)x(110)]-type electrodes. Both figures show that the current density due to ketone reduction increases with the step density.

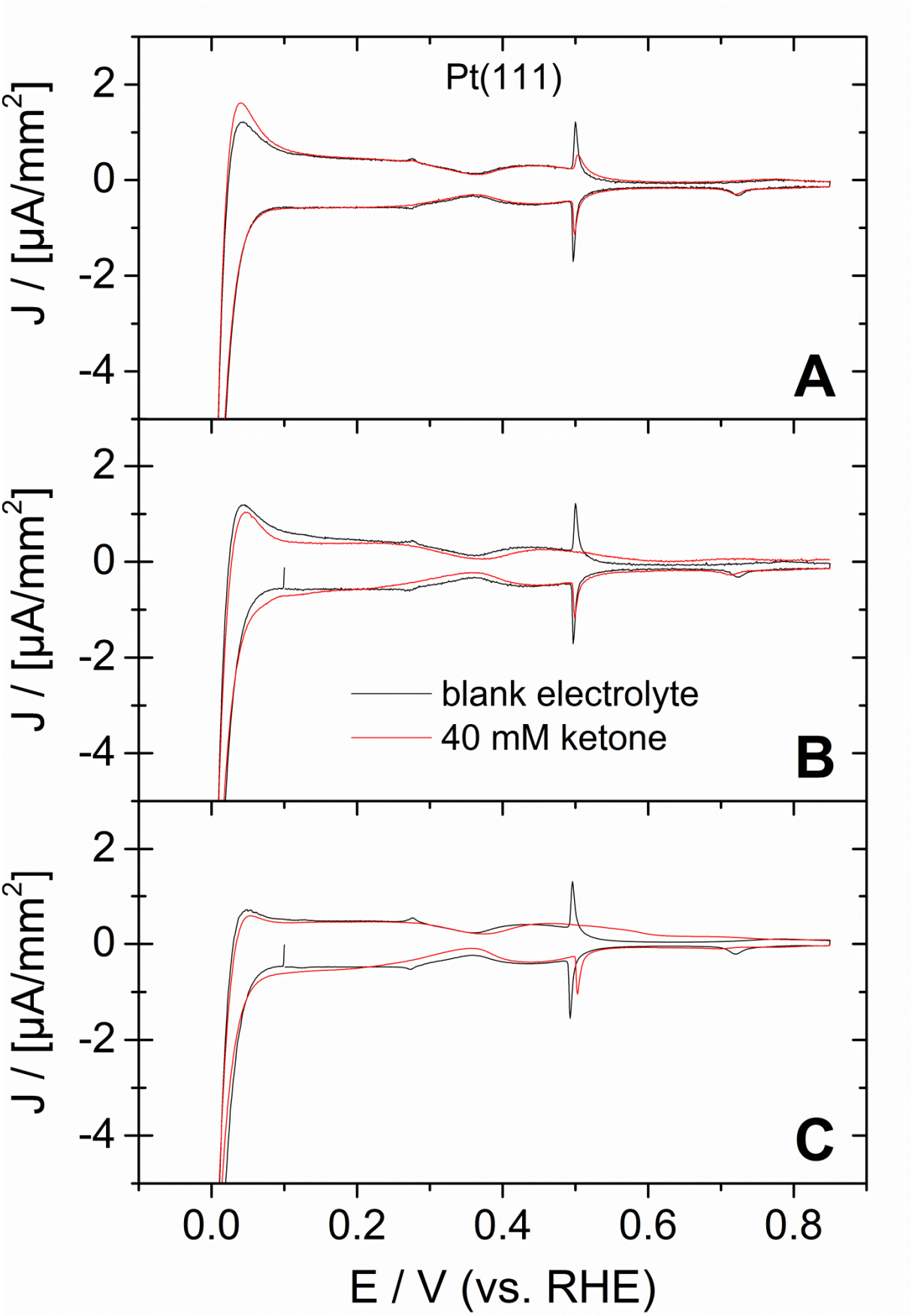


**Supplementary Figure 20. CV at Pt(111) in the presence of acetone.** Electrolyte: 0.1 M $H_2SO_4$ containing 40 mM ketone. A:Acetone; B: Butanone; C: Pentanone. Sweep rate: 0.05 V/s.

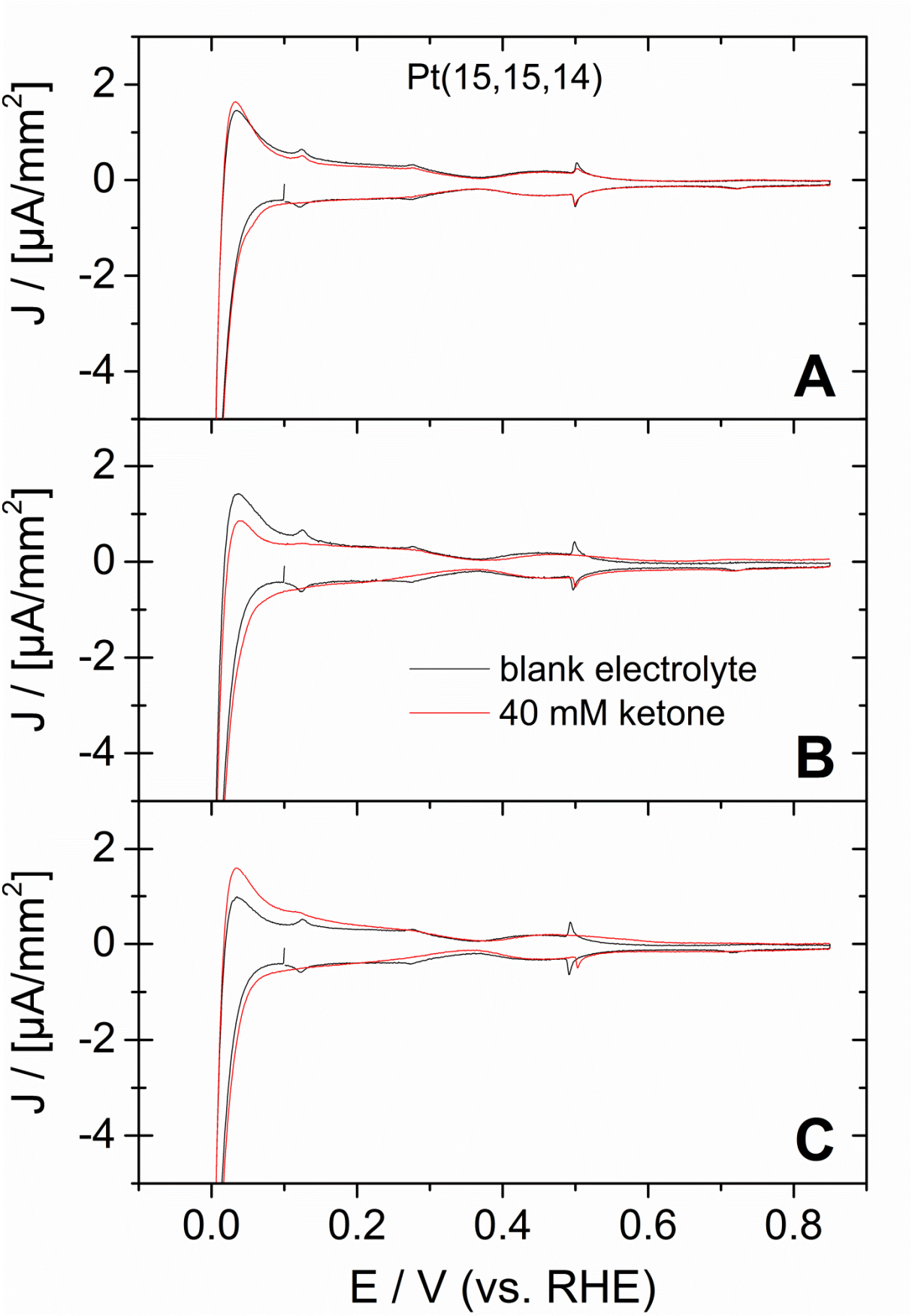


**Supplementary Figure 21. CV at Pt(15,15,14) in the presence of acetone.** Electrolyte: 0.1 M $H_2SO_4$ containing 40 mM ketone. A:Acetone; B: Butanone; C: Pentanone. Sweep rate: 0.05 V/s.

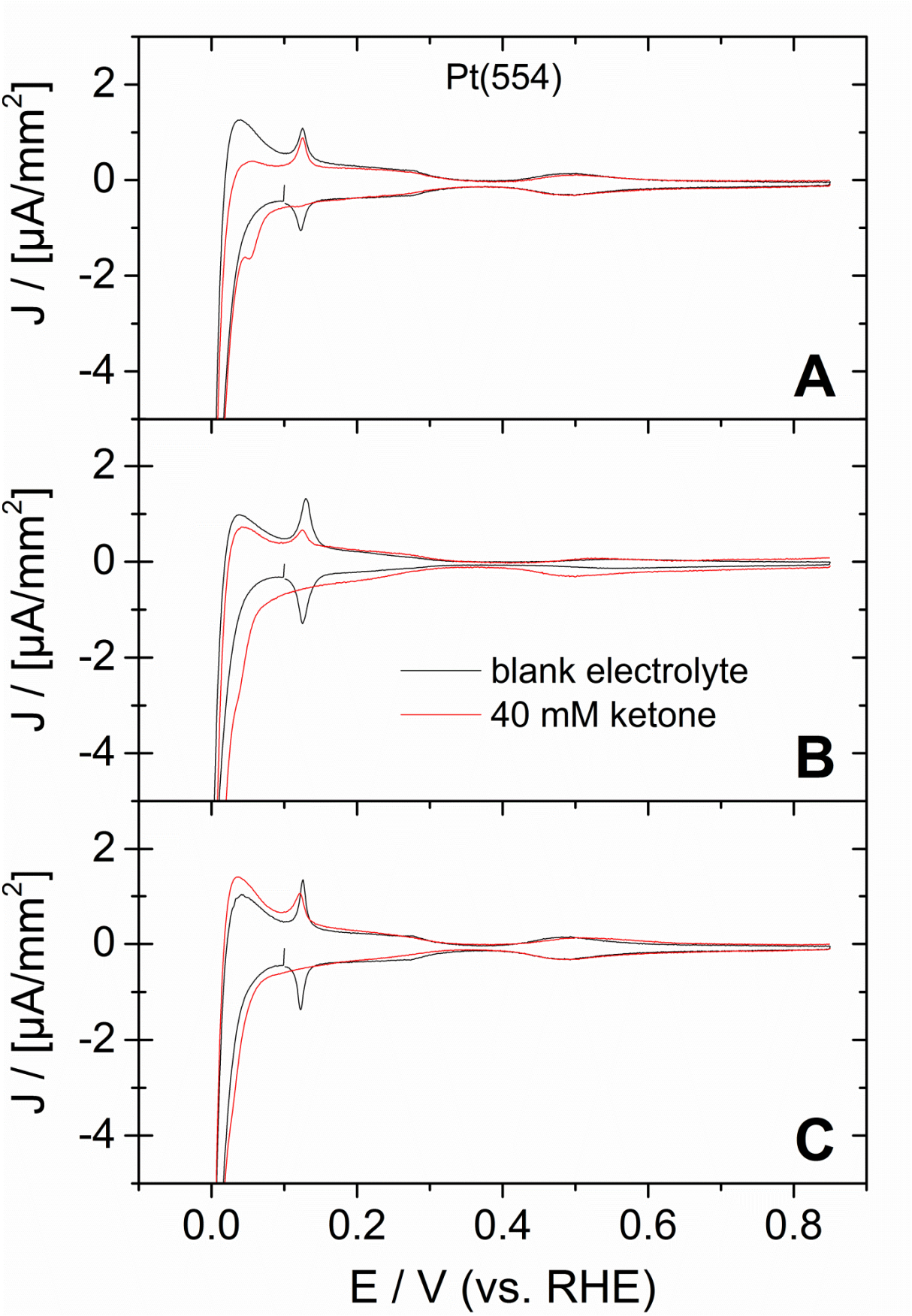


**Supplementary Figure 22. CV at Pt(554) in the presence of acetone.** Electrolyte: 0.1 M $H_2SO_4$ containing 40 mM ketone. A:Acetone; B: Butanone; C: Pentanone. Sweep rate: 0.05 V/s.

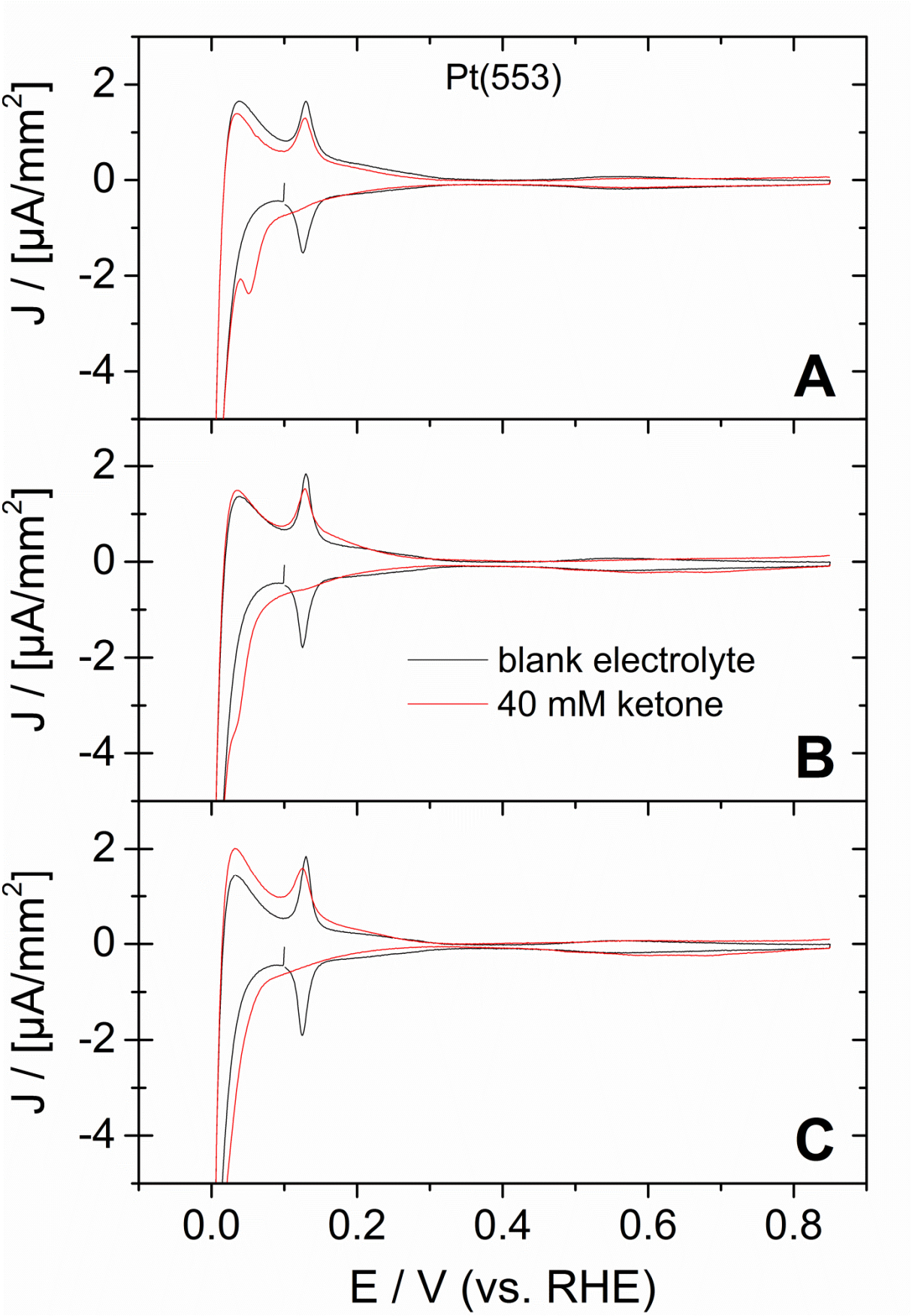


**Supplementary Figure 23. CV at Pt(553) in the presence of acetone.** Electrolyte: 0.1 M $H_2SO_4$ containing 40 mM ketone. A:Acetone; B: Butanone; C: Pentanone. Sweep rate: 0.05 V/s.

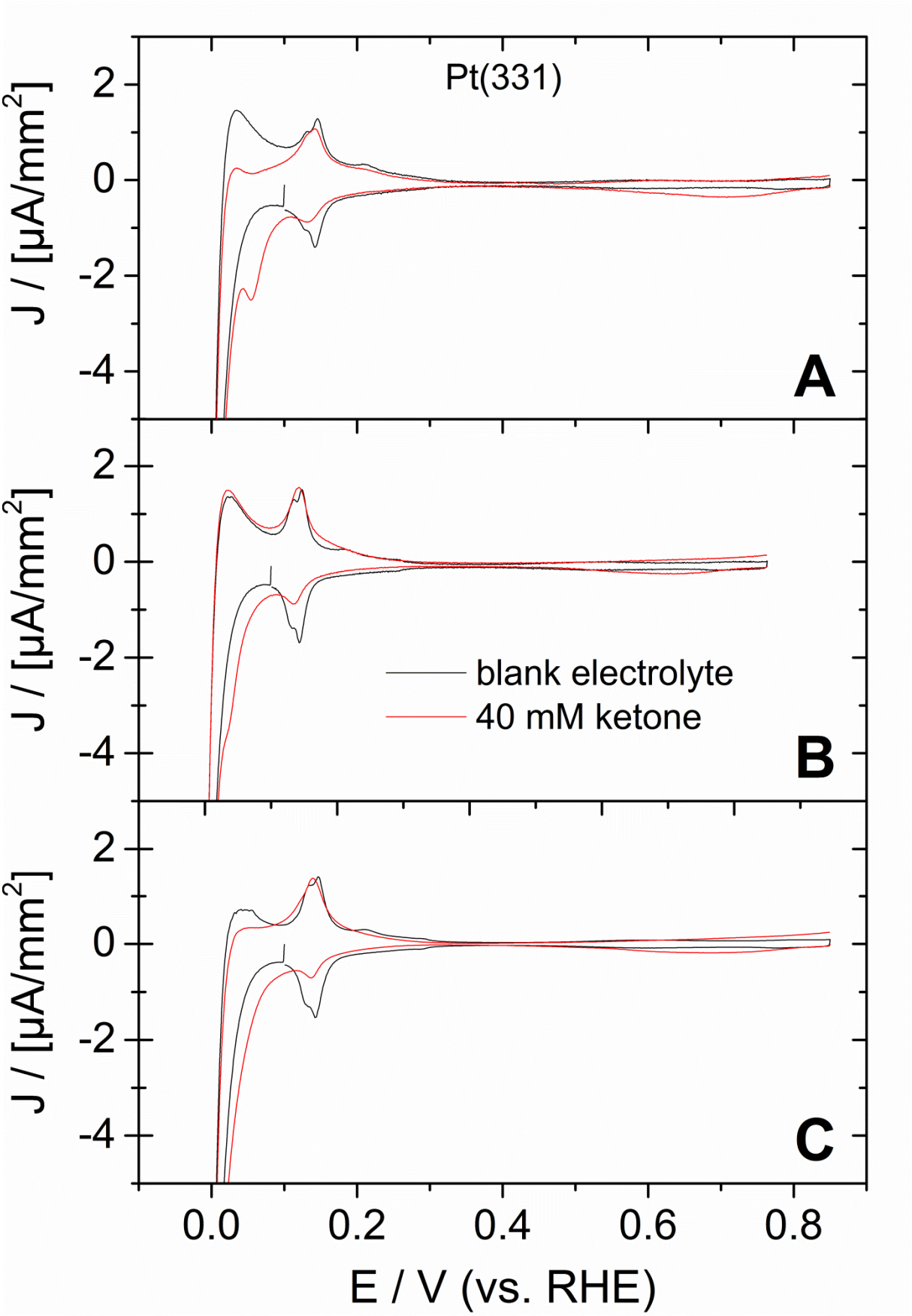


**Supplementary Figure 24. CV at Pt(331) in the presence of acetone.** Electrolyte: 0.1 M $H_2SO_4$ containing 40 mM ketone. A:Acetone; B: Butanone; C: Pentanone. Sweep rate: 0.05 V/s.

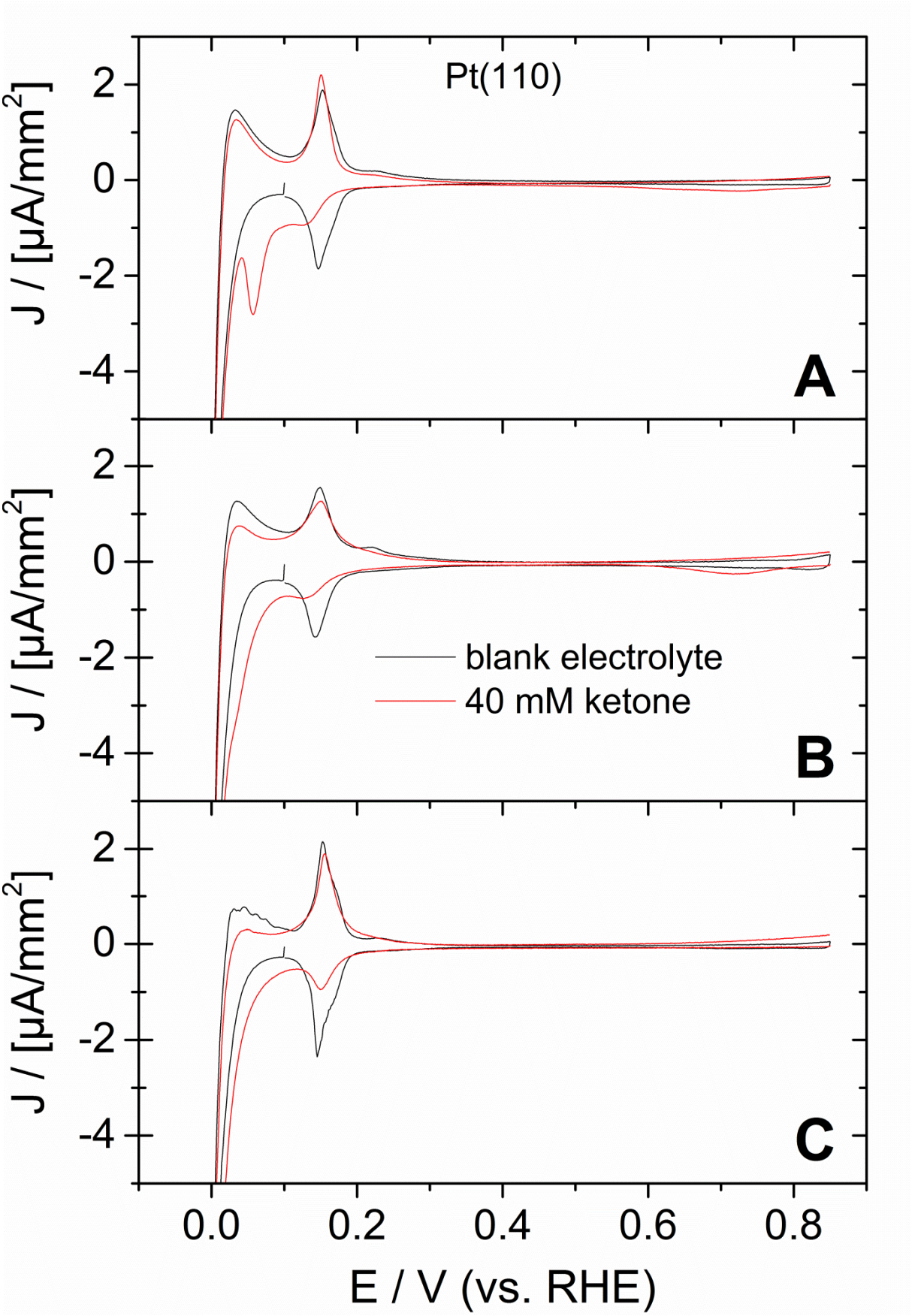


**Supplementary Figure 25. CV at Pt(110) in the presence of acetone.** Electrolyte: 0.1 M $H_2SO_4$ containing 40 mM ketone. A:Acetone; B: Butanone; C: Pentanone. Sweep rate: 0.05 V/s.

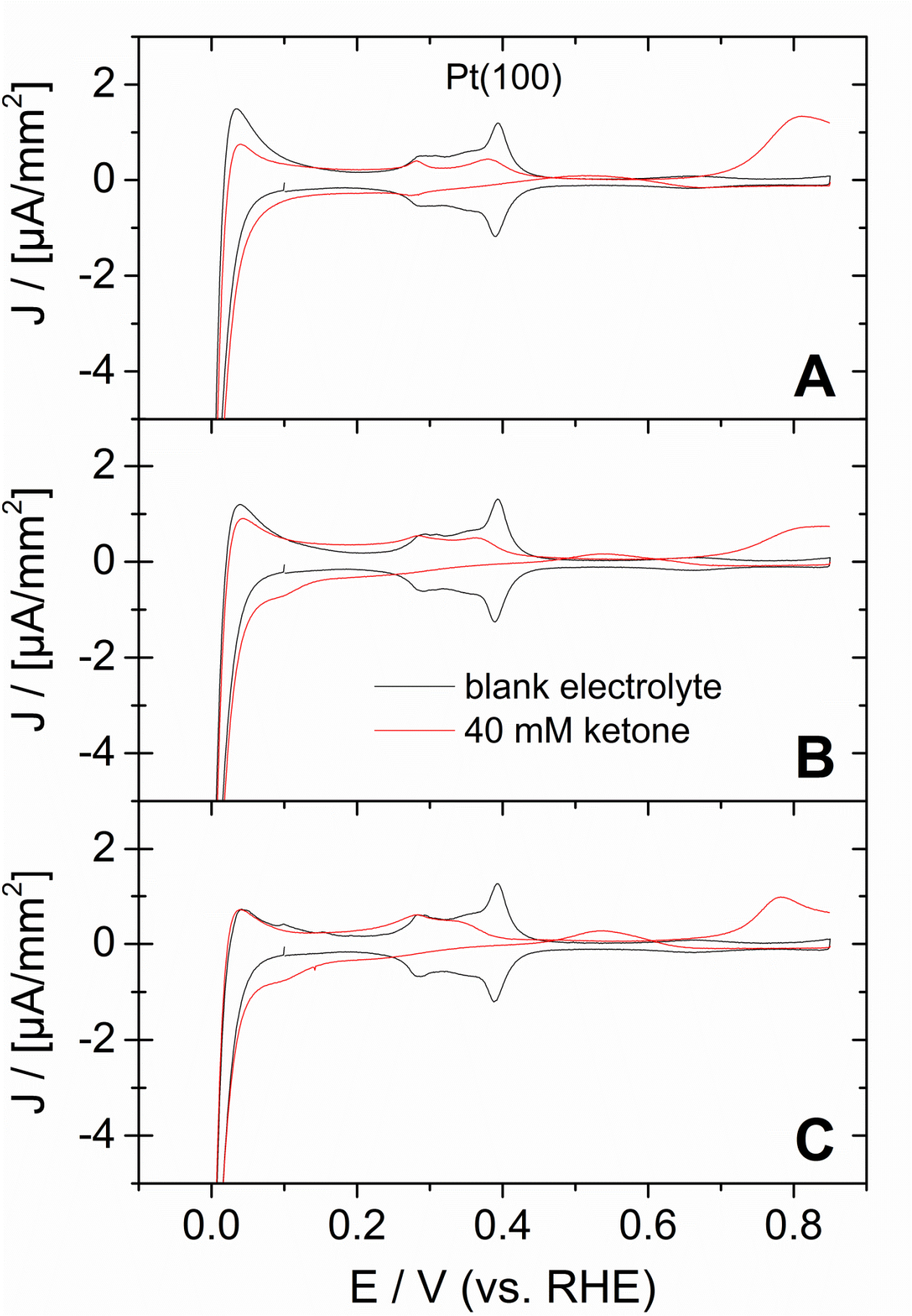


**Supplementary Figure 26. CV at Pt(100) in the presence of acetone.** Electrolyte: 0.1 M $H_2SO_4$ containing 40 mM ketone. A:Acetone; B: Butanone; C: Pentanone. Sweep rate: 0.05 V/s.

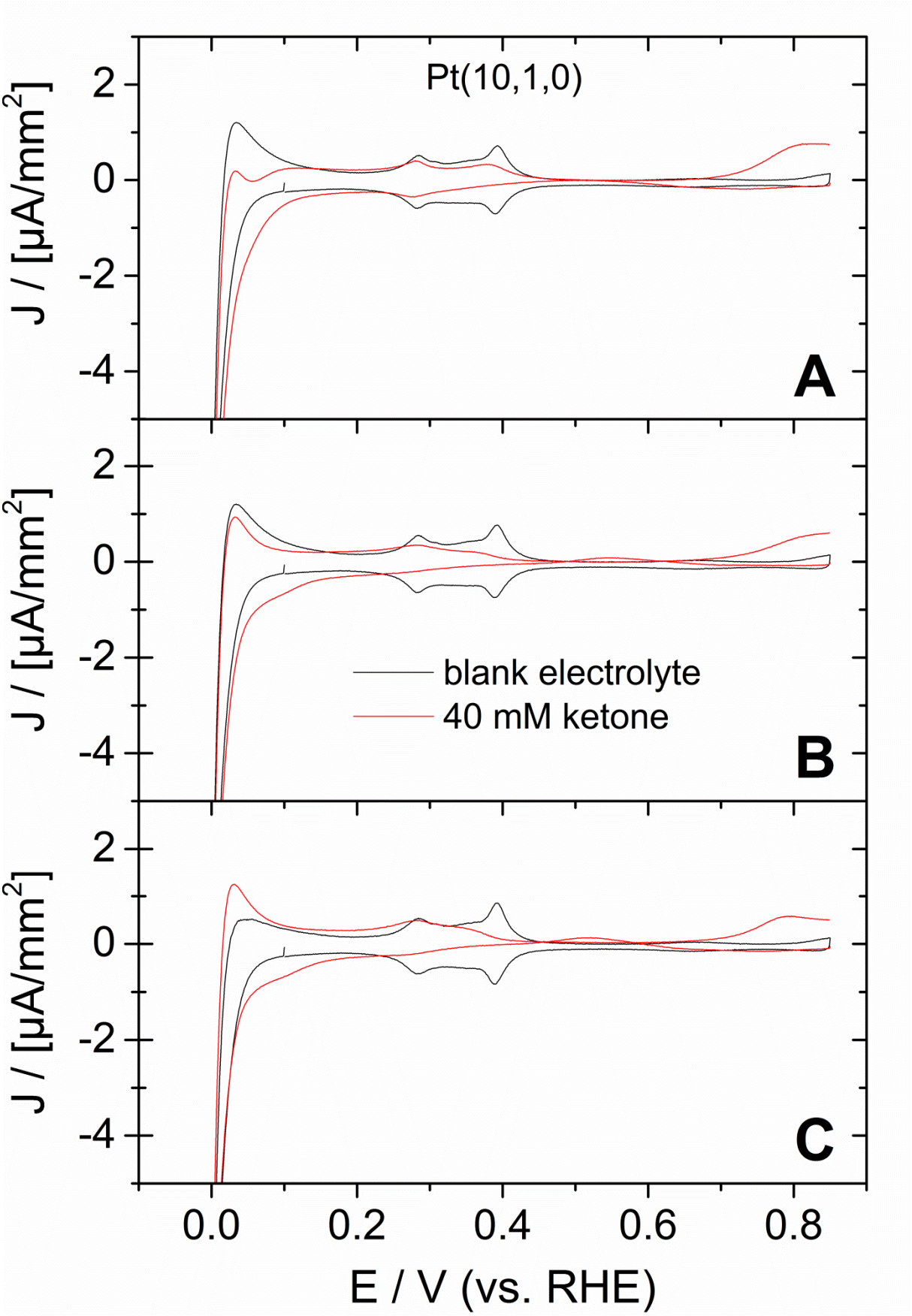


**Supplementary Figure 27. CV at Pt(10,1,0) in the presence of acetone.** Electrolyte: 0.1 M $H_2SO_4$ containing 40 mM ketone. A:Acetone; B: Butanone; C: Pentanone. Sweep rate: 0.05 V/s.

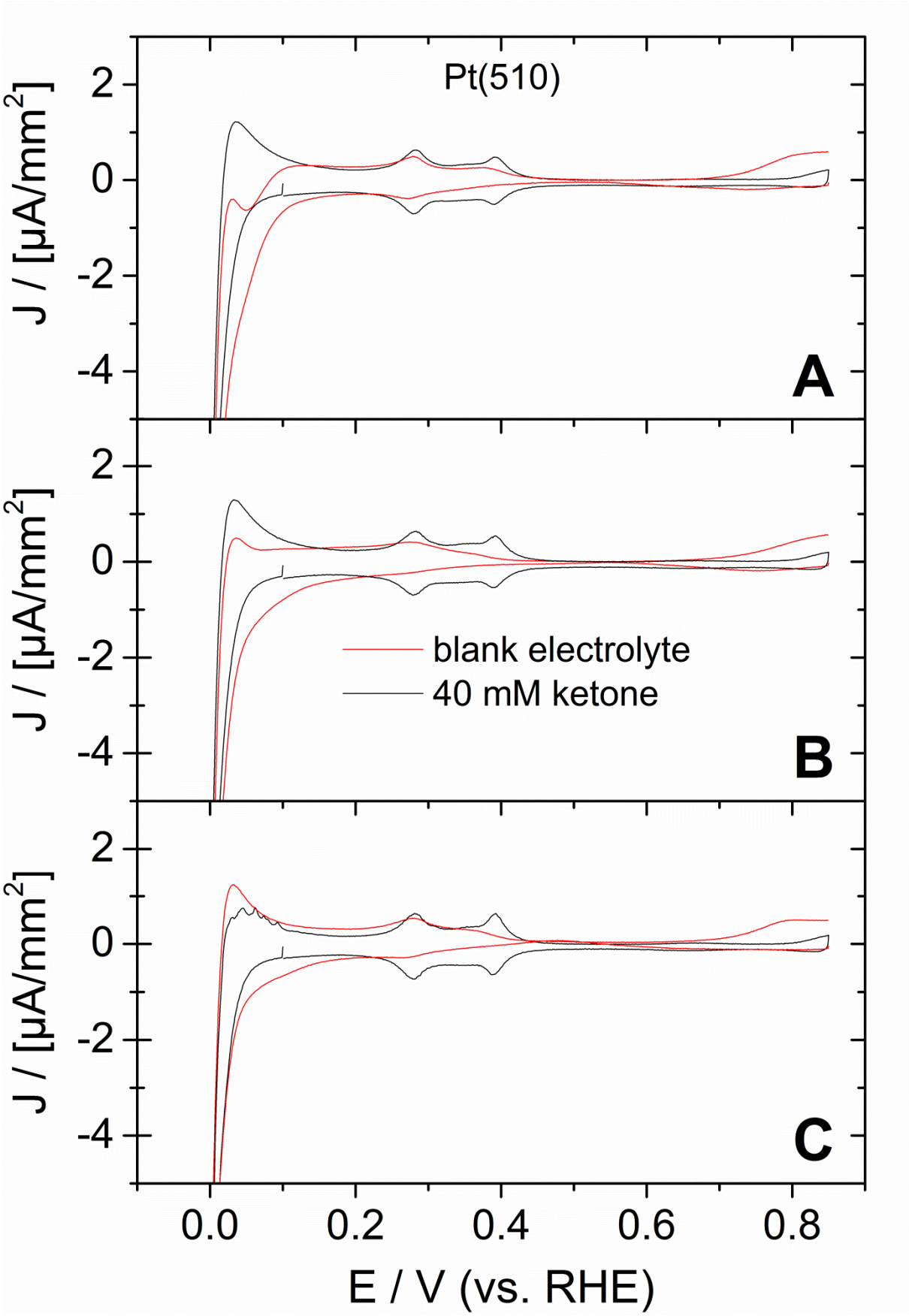


**Supplementary Figure 28. CV at Pt(510) in the presence of acetone.** Electrolyte: 0.1 M $H_2SO_4$ containing 40 mM ketone. A:Acetone; B: Butanone; C: Pentanone. Sweep rate: 0.05 V/s.

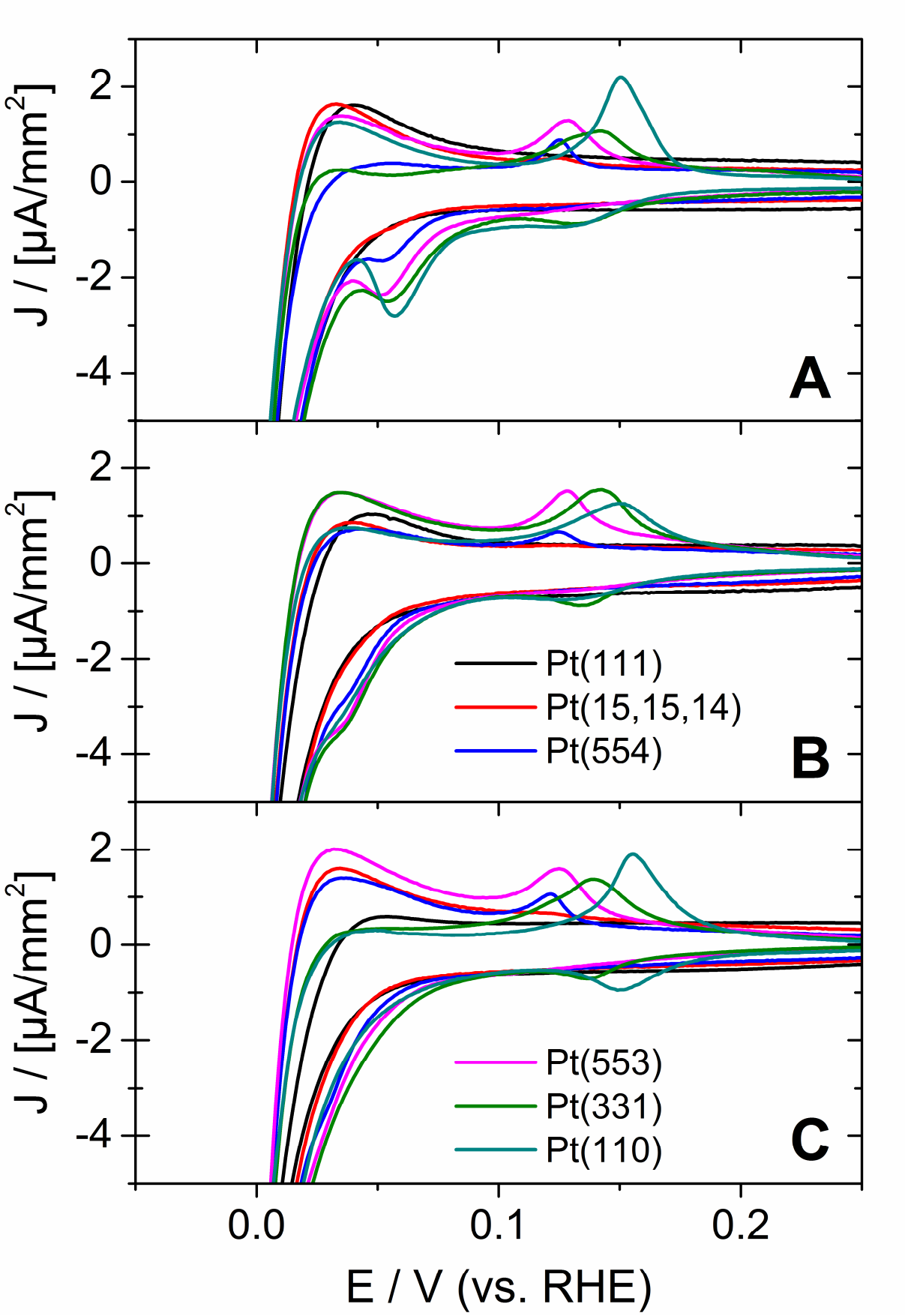


**Supplementary Figure 29. Effect of step density at Pt(111)-type electrodes on Ketone reduction.** Electrolyte 40 mM ketone containing 0.1 M $H_2SO_4$. A: Acetone; B: Butanone; C: Pentanone.

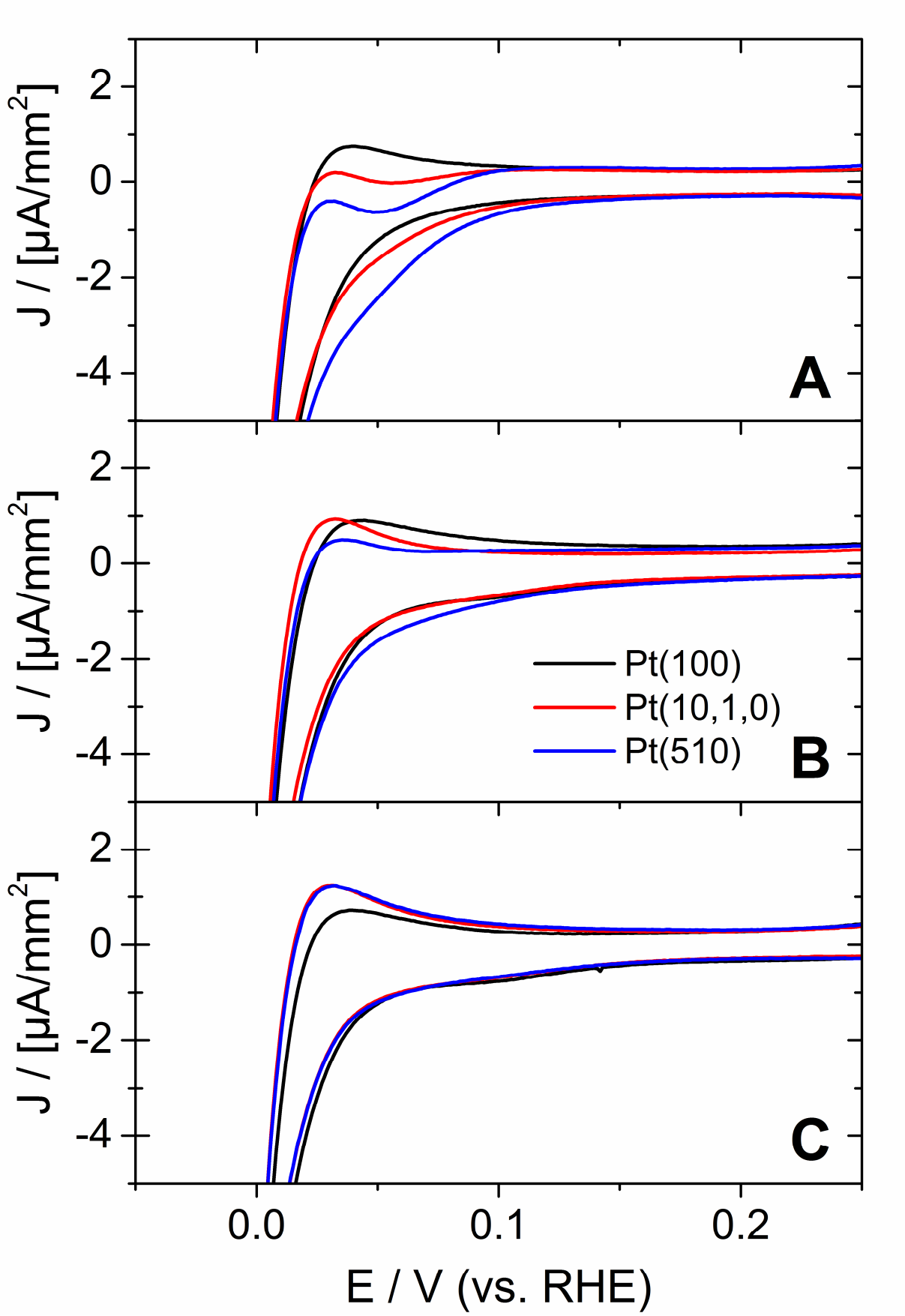


**Supplementary Figure 30. Effect of step density at Pt(100)-type electrodes on Ketone reduction. Electrolyte** 40 mM ketone containing 0.1 M $H_2SO_4$. A: Acetone; B: Butanone; C: Pentanone.

***Supplementary Note 11. OLEMS-Data for the Reduction of Butanone at Pt(100), Pt(510) and Pt(553)***

Supplementary Figure 31 shows the OLEMS response of the ionic current for mass 2 (Figure S31A, B and C) and for mass 43 (Supplementary Figure 31C, F and I) during potential steps in the potential region of ketone reduction. As mentioned in the main paper, OLEMS results have a qualitative and not a quantitative character. Among others, the geometry of the setup determines the share of products that enter the vacuum of the mass spectrometer. By geometry we mean here the distance and the angle between the tip and the surface of the electrode, which cannot be reproduced reliably from one experiment to the other. Therefore the following applies: although there is a proportionality between ionic current and molecules entering the mass spectrometer, we cannot determine how many molecules are formed in the electrochemical reaction because we do not know which share of electrochemically formed molecules actually enter the mass spectrometer. In other words, we do not know the collection efficiency for each experiment and cannot control it reproducibly.

In order to be able to compare the OLEMS data obtained in different experiments and at different electrodes, we show in Supplementary Figure 31 the ionic current for mass 2. The signal in ionic current for mass 2 is due to the evolution of hydrogen. If we assume that roughly the same amounts of hydrogen are formed at the same potential at Pt(100), Pt(510) and Pt(553) electrode, we can infer from the similar signal intensity in the ionic current for mass 2 that roughly the same share of products enters the vacuum of the mass spectrometer. Hence, we can also roughly compare the signals in the ionic current for mass 43. This mass fragment can be assigned to butane, which forms at the Pt(510) electrode when we step the potential to 0.06 V and more negative potentials. Barely any signal intensity is observed at both Pt(100) and Pt(510) electrodes. Since (100) terraces appear to be inherently inactive for the reduction of aliphatic ketones, it is not surprising that we cannot observe butane formation parallel to hydrogen evolution. In contrast, we know that the Pt(553) electrode is active for the hydrogenation of aliphatic ketones. However, significantly less butane is

formed than at the Pt(510) electrode. Also in the case of butanone reduction this leaves the alcohol as the dominant product of ketone reduction at Pt(553). We observe, therefore, the same selectivity trends with respect to surface orientation as observed for acetone.

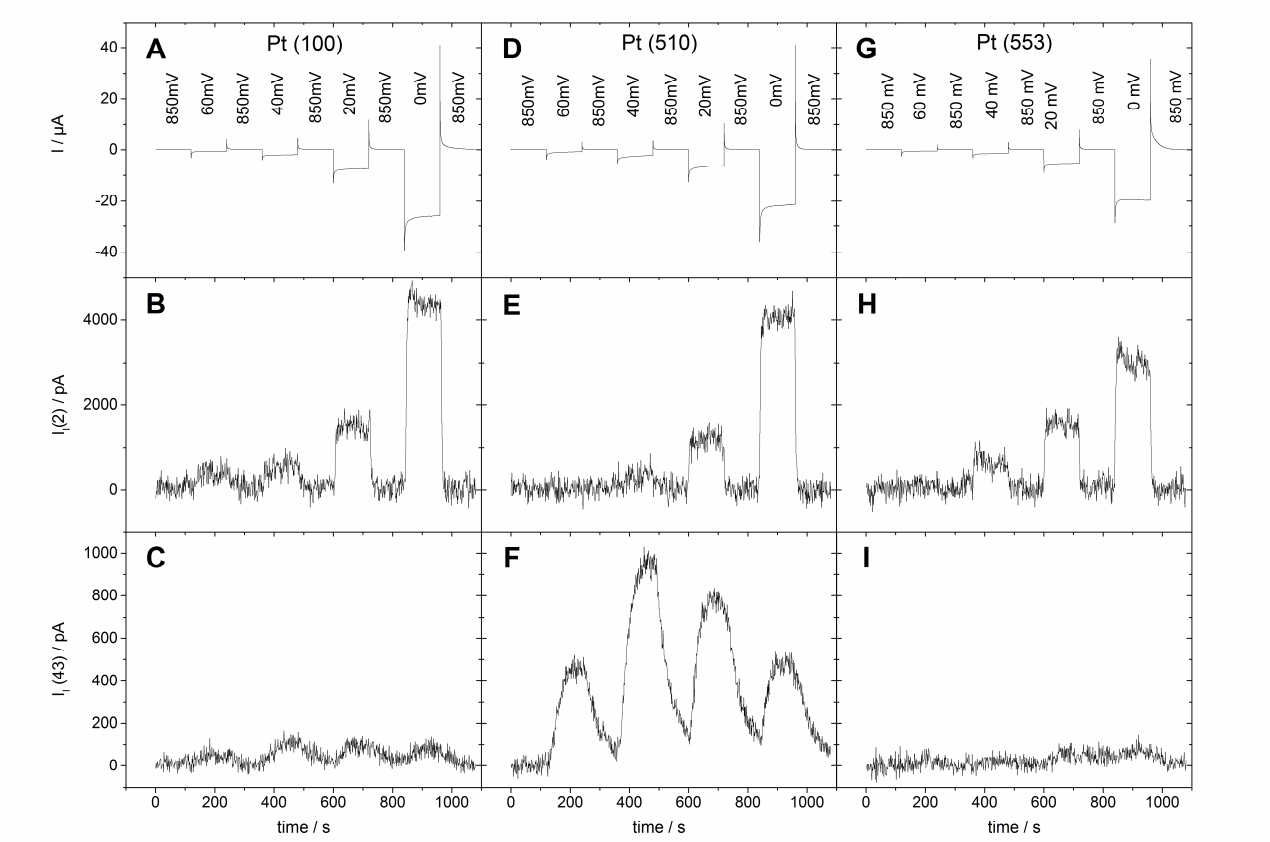


**Supplementary Figure 31. Structure sensitivity of butane formation upon butaonone reduction.** Potential steps from 0.85 V into the potential region of butanone reduction in 0.1 M butanone containing 0.1 M $H_2SO_4$. A, B and C: at Pt(100); D, E and F: at Pt(510); G, H, I: at Pt(553). A, D, G: Faradic current as a function of time. B, E and H: Ionic current for mass 2 as a function of time. Similar signal strength for hydrogen during a step to 0 V indicates similar sensitivities in the experimental setups. C, F, and I: Ionic current for mass 43. A signal in the ionic current for mass 43 indicates the formation of butane.

**Supplementary References**


1. Avery, N.R. EELS identification of the adsorbed species from acetone adsorption on Pt(111). *Surface Science* **125**, 771-786 (1983).
2. Lai, S.C.S., Kleyn, S.E.F., Rosca, V. & Koper, M.T.M. Mechanism of the Dissociation and Electrooxidation of Ethanol and Acetaldehyde on Platinum As Studied by SERS. *The Journal of Physical Chemistry C* **112**, 19080-19087 (2008).
3. Li, H. et al. Why (1 0 0) Terraces Break and Make Bonds: Oxidation of Dimethyl Ether on Platinum Single-Crystal Electrodes. *Journal of the American Chemical Society* **135**, 14329-14338 (2013).
4. Ledezma-Yanez, I., Gallent, E.P., Koper, M.T.M. & Calle-Vallejo, F. Structure-sensitive electroreduction of acetaldehyde to ethanol on copper and its mechanistic implications for CO and CO2 reduction. *Catalysis Today* **262**, 90-94 (2016).
5. Pérez-Gallent, E., Marcandalli, G., Figueiredo, M.C., Calle-Vallejo, F. & Koper, M.T.M. Structure- and Potential-Dependent Cation Effects on CO Reduction at Copper Single-Crystal Electrodes. *Journal of the American Chemical Society* **139**, 16412-16419 (2017).
6. Peterson, A.A., Abild-Pedersen, F., Studt, F., Rossmeisl, J. & Nørskov, J.K. How copper catalyzes the electroreduction of carbon dioxide into hydrocarbon fuels. *Energy & Environmental Science* **3**, 1311-1315 (2010).
7. Calle-Vallejo, F. & Koper, M.T.M. Theoretical Considerations on the Electroreduction of CO to C2 Species on Cu(100) Electrodes. *Angewandte Chemie International Edition* **52**, 7282-7285 (2013).
8. He, Z.-D., Hanselman, S., Chen, Y.-X., Koper, M.T.M. & Calle-Vallejo, F. Importance of Solvation for the Accurate Prediction of Oxygen Reduction Activities of Pt-Based Electrocatalysts. *The Journal of Physical Chemistry Letters* **8**, 2243-2246 (2017).
9. Pohl, M.D., Watzele, S., Calle-Vallejo, F. & Bandarenka, A.S. Nature of Highly Active Electrocatalytic Sites for the Hydrogen Evolution Reaction at Pt Electrodes in Acidic Media. *ACS Omega* **2**, 8141-8147 (2017).